

The MicroJy and NanoJy Radio Sky: Source Population and Multi-wavelength Properties

Paolo Padovani*

European Southern Observatory, Karl-Schwarzschild-Str. 2, D-85748 Garching bei München, Germany

Accepted ... Received ...; in original form ...

ABSTRACT

I present simple but robust estimates of the types of sources making up the faint, sub- μ Jy radio sky. These include, not surprisingly, star-forming galaxies and radio-quiet active galactic nuclei but also two “new” populations, that is low radio power ellipticals and dwarf galaxies, the latter likely constituting the most numerous component of the radio sky. I then estimate for the first time the X-ray, optical, and mid-infrared fluxes these objects are likely to have, which are very important for source identification and the synergy between the upcoming Square Kilometre Array (SKA) and its various pathfinders with future missions in other bands. On large areas of the sky the SKA, and any other radio telescope producing surveys down to at least the μ Jy level, will go deeper than all currently planned (and past) sky surveys, with the possible exception of the optical ones from the Panoramic Survey Telescope and Rapid Response System and the Large Synoptic Survey Telescope. The Space Infrared telescope for Cosmology and Astrophysics, the James Webb Space Telescope (JWST), and in particular the Extremely Large Telescopes (ELTs) will be a match to the next generation radio telescopes but only on small areas and above $\sim 0.1 - 1 \mu$ Jy (at 1.4 GHz), while even the International X-ray Observatory will only be able to detect a small (tiny) fraction of the μ Jy (nanoJy) population. On the other hand, most sources from currently planned all-sky surveys, with the likely exception of the optical ones, will have a radio counterpart within the reach of the SKA. JWST and the ELTs might turn out to be the main, or perhaps even the only, facilities capable of securing optical counterparts and especially redshifts of μ Jy radio sources. Because of their sensitivity, the SKA and its pathfinders will have a huge impact on a number of topics in extragalactic astronomy including star-formation in galaxies and its co-evolution with supermassive black holes, radio-loudness and radio-quietness in active galactic nuclei, dwarf galaxies, and the main contributors to the radio background.

Key words: galaxies: active – galaxies: dwarf – galaxies: star formation – radio continuum: general – infrared: galaxies – X-rays: galaxies

1 INTRODUCTION

The radio bright ($\gtrsim 1$ mJy) radio sky consists for the most part of active galactic nuclei (AGN) whose radio emission is generated from the gravitational potential associated with a supermassive black-hole and includes the classical extended jet and double lobe radio sources as well as compact radio components more directly associated with the energy generation and collimation near the central engine. Below 1 mJy there is an increasing contri-

bution to the radio source population from synchrotron emission resulting from relativistic plasma ejected from supernovae associated with massive star formation in galaxies. After years of intense debate, however, this contribution appears not to be overwhelming, at least down to $\sim 50 \mu$ Jy. Deep ($S_{1.4\text{GHz}} \geq 42 \mu$ Jy) radio observations of the VLA-Chandra Deep Field South (CDFS), complemented by a variety of data at other frequencies, imply a roughly 50/50 split between star-forming galaxies (SFG) and AGN (Padovani et al. 2009), in broad agreement with other recent papers (e.g., Seymour et al. 2008; Smolčić et al. 2008). About half of the AGN are

* E-mail: ppadovan@eso.org

radio-quiet, that is of the type normally found in optically selected samples and characterised by relatively low radio-to-optical flux density ratios and radio powers (Padovani et al. 2009). These objects represent an almost negligible minority above 1 mJy.

This source population issue is strongly related to the very broad and complex relationship between star formation and AGN in the Universe. At the cosmological level, the growth of supermassive black holes in AGN appears to be correlated with the growth of stellar mass in galaxies (e.g., Merloni, Rudnick & Di Matteo 2008). At the local level, the accreting gas feeding the black hole at the centre of the AGN might trigger a starburst. The black hole in turn feeds energy back to its surroundings through winds and jets, which can compress the gas and therefore accelerate star formation but can also blow it all away, thereby stopping accretion and star formation altogether. Although the details are still not entirely settled, there is however increasing evidence that in the co-evolution of supermassive black holes and galaxies nuclear activity plays a major role through the so-called “AGN Feedback” (e.g., Cattaneo et al. 2009).

Radio observations afford a view of the Universe unaffected by the absorption, which plagues most other wavelengths, and therefore provide a vital contribution to our understanding of this co-evolution. However, while we have a reasonably good handle on the radio evolution and luminosity functions (LFs) of powerful sources (e.g., radio quasars), the situation for the intrinsically fainter, and therefore more numerous, radio sources is still murky. For example, it is still not entirely clear how strongly low-luminosity, Fanaroff-Riley (FR) type I radio galaxies evolve (Gendre, Best & Wall 2010). Moreover, the widely used SFG LF of Condon (1989) is highly uncertain at the low end ($P_{1.4\text{GHz}} \lesssim 10^{20} \text{ W Hz}^{-1}$) because, although these sources are intrinsically very numerous, the volume within which they can be detected is small (their “visibility function” is very low). Indeed, a source with $P_{1.4\text{GHz}} \sim 10^{20} \text{ W Hz}^{-1}$ could be detected in the deepest radio image currently available (Owen & Morrison 2008) out to $z \sim 0.05$, but it is not (Strazzullo et al. 2010), because the survey area is too small. And already at $z \sim 1$, assuming a luminosity evolution $\propto (1+z)^3$, such a source would have a flux density as low as $\sim 0.2 \mu\text{Jy}$. Finally, there are still no published results on the radio evolution of radio-quiet AGN, which are intrinsically weak sources ($P_{1.4\text{GHz}} \lesssim 10^{24} \text{ W Hz}^{-1}$) and a non-negligible component of the sub-mJy sky. Note that faint (sub- μJy) radio sources have also been proposed by Singal et al. (2010) as the main contributors to the extragalactic radio background recently reported by the ARCADE 2 collaboration (Fixsen et al. 2010). Deeper radio observations over large areas of the sky are desperately needed to determine the LF and evolution of the most common radio sources in the Universe.

These will soon be realised, as radio astronomy is at the verge of a revolution, which will usher in an era of large area surveys reaching flux density limits well below current ones. The Square Kilometre Array (SKA)¹, in

fact, will offer an observing window between 70 MHz and 10 GHz extending well into the *nanoJy* regime with unprecedented versatility. The field of view will be large, up to $\sim 200 \text{ deg}^2$ below 0.3 GHz and possibly reaching $\sim 25 \text{ deg}^2$ at 1.4 GHz. First science with $\sim 10\%$ SKA should be near the end of this decade. Location will be in the southern hemisphere, either Australia or South Africa. Many surveys are being planned with the SKA, possibly comprising an “all-sky” 1 μJy survey at 1.4 GHz and an HI survey out to redshift ~ 1.5 , which should include $\sim 10^9$ galaxies.

The SKA will not be the only participant to this revolution. The LOw Frequency ARray (LOFAR)² has recently started operations and will carry out large area surveys at 15, 30, 60, 120 and 200 MHz (see Morganti et al. 2009, for details), opening up a whole new region of parameter space at low radio frequencies. Many other radio telescopes are currently under construction in the lead-up to the SKA including the Expanded Very Large Array (EVLA)³, the Australian Square Kilometre Array Pathfinder (ASKAP)⁴, the Allen Telescope Array⁵, Apertif⁶, and Meerkat⁷. These projects will survey the sky vastly faster than is possible with existing radio telescopes producing surveys covering large areas of the sky down to fainter flux densities than presently available.

Current deep surveys include a number of VLA small area surveys below 0.1 mJy at a few GHz, reaching a maximum area of $\sim 2 \text{ deg}^2$ (VLA-COSMOS; Bondi et al. 2008) and a minimum flux density $\sim 15 \mu\text{Jy}$ at 1.4 GHz (SWIRE; Owen & Morrison 2008) and $\sim 7.5 \mu\text{Jy}$ at 8.4 GHz (SA 13; Fomalont et al. 2002). The NRAO VLA Sky Survey (NVSS; Condon et al. 1998) and the Faint Images of the Radio Sky at Twenty centimeters (FIRST; Becker et al. 1995) only reach 1.4 GHz limits of 2.5 and 1 mJy respectively but cover much larger areas (82% and 22% of the sky respectively).

What lies beneath the surface of the deepest surveys we currently have? Predictions for the source population at radio flux densities $< 1 \mu\text{Jy}$ have been made, amongst others, by Hopkins et al. (2000), Windhorst (2003), Jackson (2004), Jarvis & Rawlings (2004), and Wilman et al. (2008). These papers have presented detailed estimates for the number counts of faint radio sources predicting, for example, that SFG should make up $\sim 90\%$ of the total population at $S_{1.4\text{GHz}} \sim 1 \mu\text{Jy}$ (Wilman et al. 2008) but had to rely, for obvious reasons, on extrapolations. Only the last two papers include radio-quiet AGN in their modelling by converting their X-ray LF to the radio band assuming a linear correlation between radio and X-ray powers. Most importantly, as described below, two crucial constituents of the sub- μJy sky have been excluded by all of these studies.

The first aim of this paper is then to have a broad look at the likely astrophysical populations, which make

¹ <http://www.skatelescope.org>

² <http://www.astron.nl/radio-observatory/astronomers/lofar-astronomers>

³ <http://science.nrao.edu/evla>

⁴ <http://www.atnf.csiro.au/projects/askap/>

⁵ <http://ral.berkeley.edu/ata>

⁶ <http://www.astron.nl/general/apertif/apertif>

⁷ <http://www.ska.ac.za/meerkat>

up the very faint radio sky. But detecting sources is only part of the story, as then comes the identification process. This requires a wealth of multi-wavelength data, ranging from the optical/near-IR imaging needed to provide an optical counterpart and, when needed, photometric redshifts, to the optical/near-IR spectra required to estimate a redshift, and hence the distance of sources, to the X-ray data, which are vital to separate AGN from SFG (e.g., Padovani et al. 2009, and references therein), to the mid-infrared colours, which provide additional information on this separation (e.g., Sajina, Lacy & Scott 2005). The second goal of this work is then to provide estimates for the the X-ray, optical, and mid-infrared fluxes these sources are likely to have. Optical magnitudes will also determine how feasible it will be to obtain redshifts for them. This kind of information is important for planning purposes, to be ready to take full advantage of the new, deep radio data, and also to maximise the synergy between the SKA and its pathfinders, and present but also, most importantly, future missions. To the best of my knowledge, these estimates have never been made before.

Throughout this paper spectral indices are written $S_\nu \propto \nu^{-\alpha}$, magnitudes are in the AB system, and the values $H_0 = 70 \text{ km s}^{-1} \text{ Mpc}^{-1}$, $\Omega_M = 0.3$, and $\Omega_\Lambda = 0.7$ have been used, unless otherwise noted. All the radio results refer to 1.4 GHz. Although I mention only the SKA throughout the paper, my results obviously apply to any other radio telescope producing surveys reaching the μJy level. I also make reference to a large number of missions and projects, for which I give mainly sensitivity information. Readers wanting to know more should consult the relevant World Wide Web pages, whose addresses are provided in the text.

2 MICROJY AND NANOJY RADIO SOURCE POPULATION

I present here a simple approach to study the radio sky source population, based on only two parameters: the smallest flux density and the largest surface density of radio sources. The main idea is to provide robust results based on some basic observables and to pay particular attention to *all* populations reaching below the μJy level.

The smallest flux density f_{lim} of a population of sources depends on the minimum radio power at $z \sim 0$, $P_{\text{min}}(0)$, the maximum redshift of the sources, z_{max} , and any luminosity evolution $le(z)$, where $P(z) = P(0) \times le(z)$. If evolution peaks at $z_{\text{top}} (\leq z_{\text{max}})$ and then stops, then

$$f_{\text{lim}} = \frac{P_{\text{min}}(0)le(z_{\text{top}})(1+z_{\text{max}})^{1-\alpha}}{4\pi D_L^2(z_{\text{max}})} \quad (1)$$

where $D_L(z)$ is the luminosity distance. Luminosity evolution makes sources brighter and therefore increases f_{lim} .

The largest surface density of a population, $N(> f_{\text{lim}})$, depends on its number density at $z \sim 0$, $N_T(0)$, the maximum redshift z_{max} , and any density evolution $de(z)$, where $N_T(z) = N_T(0) \times de(z)$. Then

$$N(> f_{\text{lim}}) = \frac{N_T(0)}{4\pi} \int_0^{z_{\text{max}}} de(z) dV/dz \text{ sr}^{-1} \quad (2)$$

where dV/dz is the derivative of the comoving volume. In case of no density evolution $N(> f_{\text{lim}}) = N_T(0)V(z_{\text{max}})/4\pi \text{ sr}^{-1}$.

Information on the local LF, needed to derive $N_T(0)$ and $P_{\text{min}}(0)$, and the evolution for various classes was derived from a variety of sources. Namely:

(i) the LF for SFG is that of Sadler et al. (2002), which at the low end is complemented by that of Condon (1989); luminosity and density evolution and z_{top} are from Hopkins (2004);

(ii) the LF for radio-quiet AGN is built using data from Rush et al. (1996) ($12\mu\text{m}$ and CfA Seyfert samples) and Padovani et al. (in preparation: VLA-CDFS sample). Evolution is from Padovani et al. (in preparation), while z_{top} is from the X-ray band (Hasinger, Miyaji, & Schmidt 2005);

(iii) the LF for FR Is derives from that of Urry & Padovani (1995), which agrees well with the very recent derivation of Gendre, Best & Wall (2010) apart from the first bin; the LF was then modified accordingly and the values of $N_T(0)$ and $P_{\text{min}}(0)$ were derived. Gendre, Best & Wall (2010) find evidence of evolution for FR Is but only at $P_{1.4\text{GHz}} \gtrsim 10^{25} \text{ W Hz}^{-1}$. Since the total surface density in eq. 2 depends on the most numerous, and therefore least luminous, sources (which reach $P_{1.4\text{GHz}} \sim 10^{23} \text{ W Hz}^{-1}$) no evolution was assumed;

(iv) the LF for FR IIs is also based on that of Urry & Padovani (1995), which agrees quite well with that of Gendre, Best & Wall (2010) down to $P_{1.4\text{GHz}} \approx 10^{24} \text{ W Hz}^{-1}$. Below this value the LF is basically undetermined so no modification was done. Evolution was taken from Urry & Padovani (1995);

(v) the LF for flat-spectrum radio quasars (FSRQs), steep-spectrum radio quasars (SSRQs), and BL Lacs are based on those of Urry & Padovani (1995), which were calculated from those of FR IIs and FR Is respectively, based on a beaming model. These have been shown to agree with LFs derived from recent samples (Padovani et al. 2007). Since the FR I LF was modified, the beamed LF for BL Lacs was also changed accordingly at low powers before deriving $N_T(0)$ and $P_{\text{min}}(0)$. Evolutionary parameters are from Urry & Padovani (1995), while z_{top} values for FSRQs, SSRQs, and FR IIs⁸ come from de Zotti et al. (2005).

Values of z_{max} were fixed to the highest redshift of the class under consideration, that is ~ 6 , 6.5, and 5.5 for SFG, radio-quiet AGN, and FSRQs, SSRQs, and FR IIs respectively, apart from FR Is and BL Lacs, for which $z_{\text{max}} = 3$ was assumed. Finally, the blazar catalogue of Massaro et al. (2009) and the AGN catalogue of Padovani et al. (1997) were checked to see if any sources had radio power below the adopted P_{min} values. None was found.

Table 1 summarises the parameters used in eqs. 1 and 2. $N_T(0)$ values were derived in most cases from simple fits to the LF and should be considered approximate.

⁸ According to unified schemes (see, e.g., Urry & Padovani 1995), SSRQs and FR IIs, being FSRQs seen at larger angles with respect to the line of sight, need to share the same z_{top} .

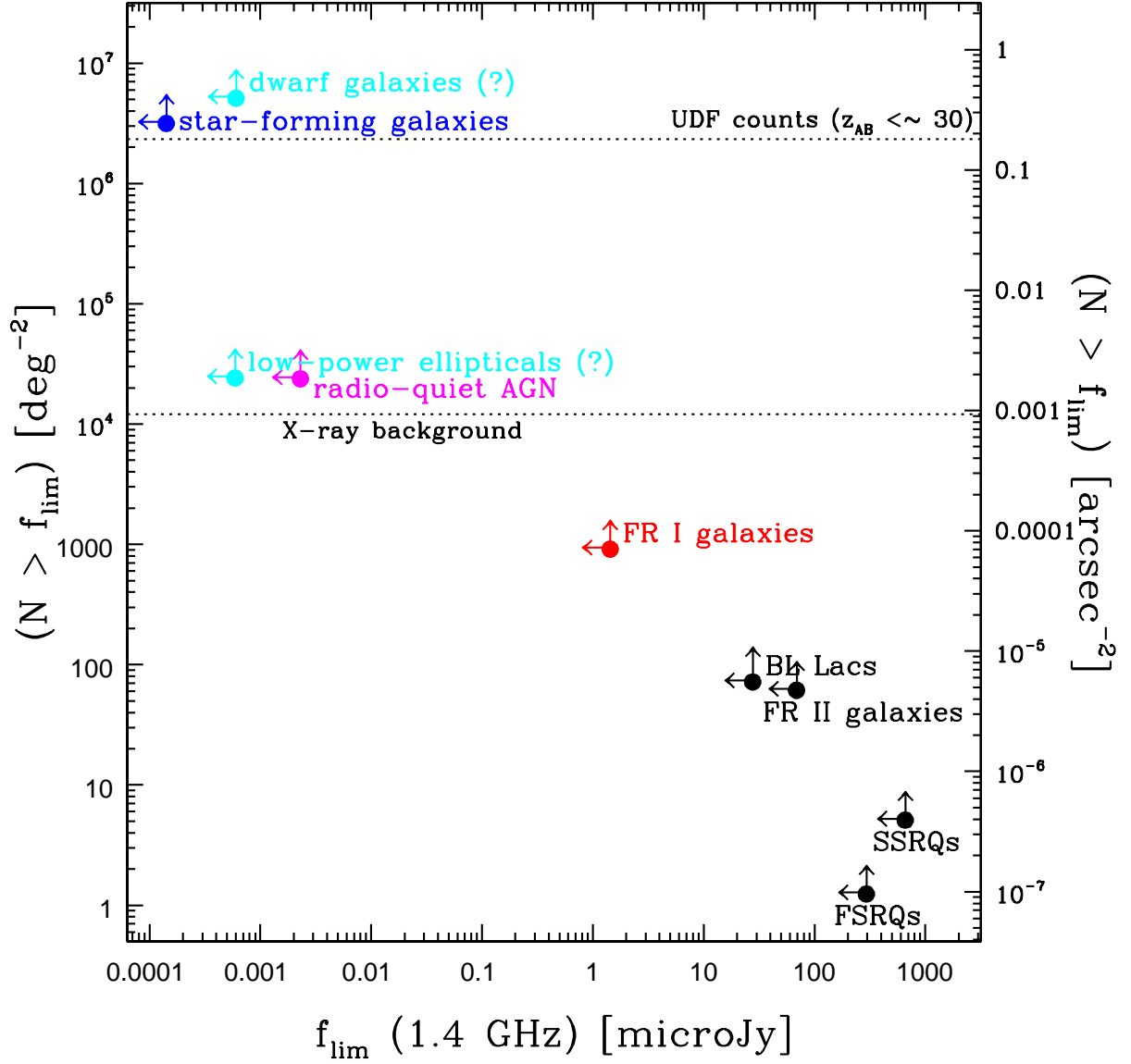


Figure 1. The largest surface density vs. the smallest flux density for various classes of radio sources. The two horizontal lines denote, from top to bottom, the surface density of the optical sources in the Hubble Ultra Deep Field and the surface density of the AGN needed to explain the X-ray background. See text for more details.

Table 1. Radio populations parameters

Class	$N_{\text{T}}(0)$ Gpc^{-3}	$P_{\text{min}}(0)$ W Hz^{-1}	LE	DE	z_{top}	z_{max}
FSRQs	12	2×10^{24}	$\exp[T(z)/0.23]^a$...	2.25	5.5
SSRQs	59	3×10^{24}	$\exp[T(z)/0.15]^a$...	2.25	5.5
FR IIs	590	3×10^{24}	$\exp[T(z)/0.26]^a$...	2.25	5.5
BL Lacs	2,310	10^{23}	$\exp[T(z)/0.32]^a$	3.0
FR Is	29,300	10^{23}	3.0
RQ AGN	3.9×10^5	5×10^{19}	$(1+z)^{2.4}$...	1.7	6.5
SFGs	4.5×10^7	2×10^{18}	$(1+z)^{2.7}$	$(1+z)^{0.15}$	2.0	6.0
Dwarf Galaxies	2.0×10^8	$< 2 \times 10^{18}$	$(1+z)^{2.7}$...	2.0	3.0
Low-power Ellipticals	4.8×10^6	$< 3 \times 10^{19}$...	$(1+z)^{-1.7}$...	3.0

^a $H_0 = 50$, $q_0 = 0$; $T(z)$ is the look-back time

The $N_T(0)$ and $P_{\min}(0)$ values from Urry & Padovani (1995) have been converted to $H_0 = 70$ from $H_0 = 50$ while the evolutionary parameters still refer to an $H_0 = 50$, $q_0 = 0$ cosmology (as a simple conversion in this case is not possible). Note that, although more complex evolutionary models than those used here have been adopted in the literature for “classical” powerful radio sources, the consensus is that such sources reach only the \approx mJy level (e.g., Jackson 2004; Wilman et al. 2008). This is in agreement with my own results below and in any case well above the flux densities of interest here.

The resulting flux and surface density limits are shown in Fig. 1. These values should be considered as robust upper and lower limits respectively, because: 1. one cannot exclude that lower-power, and therefore more numerous, objects exist; 2. z_{\max} could be larger than assumed. The latter parameter has a stronger influence on flux than on surface density. For example, for $z_{\max} = 6$, eq. 1 shows that the former value decreases by a factor $(4/7)^{1-\alpha_r} [D_L(6)/D_L(3)]^2 \sim 4.4$ ($\alpha_r = 0.7$) as compared to $z_{\max} = 3$, while from eq. 2 and in the case of no density evolution the latter increases by a factor $V(6)/V(3) \sim 2.2$. If z_{\max} increases from 6 to 10, the two values are instead ~ 2.8 and ~ 1.5 .

Fig. 1 shows that the most powerful radio sources, that is FRSQs, SSRQs, and FR IIs are, not surprisingly, the ones having the largest flux density ($\approx 0.1 - 1$ mJy) and the smallest surface density ($\approx 1 - 50$ deg $^{-2}$) limits. BL Lacs are only slightly fainter than FR IIs, while FR Is are the only radio-loud sources reaching ≈ 1 μ Jy. Radio-quiet AGN and SFG are the faintest classes, going into the nanoJy regime, with SFG dominating the faint radio sky (amongst “classical” radio sources: see below). Indeed, the differential counts of Wilman et al. (2008) predict a strong dominance ($\sim 90\%$) of SFG at 1 μ Jy, which gets slightly weaker at nanoJy flux densities.

In Fig. 1 I have also plotted two horizontal lines. The one at $N \approx 10^4$ deg $^{-2}$ denotes the surface density of the AGN needed to explain the X-ray background (Gilli, private communication, based on Gilli et al. 2007). Since these for the most part are radio-quiet AGN, its proximity to the estimated surface density of this class is reassuring. The other line at $N \approx 2 \times 10^6$ deg $^{-2}$ indicates the surface density of the optical sources in the Hubble Ultra Deep Field (UDF) (Beckwith et al. 2006), thought to be mostly star-forming galaxies. The fact that this is very close to the completely independent estimate for SFG in the radio band shows that the latter is perfectly plausible.

I argue that two other populations play a major role at $S_{1.4\text{GHz}} < 1$ μ Jy. The first one is that of low-power ellipticals. It has been known for quite some time that ellipticals of similar optical luminosity vary widely in radio power, with some (non-dwarf) galaxies having $P_{5\text{GHz}} < 2 \times 10^{19}$ W Hz $^{-1}$ (e.g., Sadler, Jenkins & Kotanyi 1989, converting from their cosmology). More recently, Capetti et al. (2009) have shown that 82% of early-type galaxies in the Virgo cluster with $B_T < 14.4$ are undetected at a flux density limit of ~ 0.1 Jy, which implies core radio powers $P_{8.4\text{GHz}} < 4 \times 10^{18}$ W Hz $^{-1}$. Miller et al. (2009) have studied the radio LF in the Coma cluster and found that 58% of red sequence galaxies with $M_r \leq -20.5$ are undetected

at about 28 μ Jy r.m.s. Stacking these sources, they obtained a detection corresponding to $P_{1.4\text{GHz}} \sim 3 \times 10^{19}$ W Hz $^{-1}$. These faint ellipticals are *not* represented in previous models of the sub- μ Jy sky: for example, the lower limit of the radio-loud AGN LF in Wilman et al. (2008) is $P_{1.4\text{GHz}} = 2 \times 10^{20}$ W Hz $^{-1}$. We have no information on the evolution of these radio sources but, based on the results of low-power ($P_{1.4\text{GHz}} < 10^{25}$ W Hz $^{-1}$) radio galaxies (e.g., Gendre, Best & Wall 2010, and references therein), it seems plausible to assume no luminosity evolution. Taking $P_{\min} < 3 \times 10^{19}$ W Hz $^{-1}$ and $z_{\max} = 3$ one derives $f_{\text{lim}} < 0.6$ nanoJy (assuming the same luminosity evolution as found by Cimatti, Daddi & Renzini (2006) for ellipticals in the B-band one would instead get $f_{\text{lim}} < 5$ nanoJy). (Note that since we only have an upper limit on P_{\min} in this case f_{lim} is an even more robust upper limit than for the previously discussed classes.)

As regards their surface density, I have taken the number density of all early-type galaxies from the LF in de Lapparent et al. (2003) (the two-wing Gaussian fit for $R_c \leq 21.5$ in their Tab. 7), which agrees within $\sim 20\%$ with the Schechter fit to the local Sloan Digital Sky Survey (SDSS) LF done by Bell et al. (2004). Kriek et al. (2008) have recently suggested a decrease of a factor ~ 8 in the number density of high-mass ($> 10^{11} M_\odot$) early-type galaxies between $z \sim 0$ and 2.3. Cimatti, Daddi & Renzini (2006) have found a similar trend for low-mass ($< 10^{11} M_\odot$) early-type galaxies between $z \sim 0$ and 1.2. Assuming that all ellipticals are radio sources at some (very low) level, such a density evolution, and $z_{\max} = 3$, I get from eq. 2 a limiting surface density for low-power ellipticals $\approx 2.4 \times 10^4$ deg $^{-2}$, of the same order as that of radio-quiet AGN.

The other population missing from previous studies is that of dwarf galaxies, which are very faint and constitute the most numerous extragalactic population. This class includes dwarf spheroidals and ellipticals, dwarf irregulars, and blue compact dwarf galaxies (BCDs), and it has never been considered for the simple reason that its radio LF and evolution has never been determined. But the simple approach adopted here can provide us with some idea of how faint and how numerous these sources are going to be in the sub- μ Jy sky.

The determination of the LF of dwarf galaxies is not an easy task as it requires a thorough understanding of selection effects, due to their low surface brightness. The LF appears also to be environment-dependent (e.g., Ferguson & Sandage 1991). I have taken the SDSS LF of Blanton et al. (2005), which is corrected for surface brightness incompleteness, and derived the number density of dwarf galaxies (defined by $M_r \lesssim -18.8$ [equivalent to $M_B \lesssim -18.1$], which is where there is an upturn in the slope of the LF). Available data are consistent with no density evolution at the faint end of the LF up to at least $z \approx 3$ (e.g., Cooray 2005; Salimbeni et al. 2008). With these assumptions I derive from eq. 2 a (likely) conservative limiting surface density $\approx 5 \times 10^6$ deg $^{-2}$, higher than all other classes.

As regards flux density, Leroy et al. (2005) have shown that $P_{\min, 1.4\text{GHz}}$ for dwarf galaxies is $< 1.6 \times 10^{18}$ W Hz $^{-1}$. Since most galaxies at the faint end of the LF are blue (e.g., Blanton et al. 2005; Salimbeni et al. 2008),

most dwarfs in the Universe should be of the star-forming type and I then assume the same luminosity evolution as for SFG. For $z_{\max} = 3$ I then get $f_{\text{lim}} < 0.6$ nanoJy (no evolution would imply $f_{\text{lim}} < 0.03$ nanoJy). (As was the case for low-power ellipticals, since we only have an upper limit on P_{\min} f_{lim} is an extremely robust upper limit.) In summary, *dwarf galaxies are likely to be the most numerous component of the faint radio sky.*

Although this paper deals with extragalactic sources, one might worry that stellar objects could also contribute substantially to the μJy and nanoJy sky. This is extremely unlikely. The radio thermal component of the Sun at the distance of α Centauri would have a flux density $\sim 5 - 30 \mu\text{Jy}$ (White 2004) (where the lower value refers to the quiet state and the higher one to the flaring one), which means $\sim 0.7 - 4$ nanoJy at 10 Kpc. Moreover, a Sun-like star at 10 Kpc would have a non-thermal flux density ~ 0.001 nanoJy (Seaquist 1997). Given that the most common main-sequence stars are of the M type, which are more than one order of magnitude less luminous than the Sun, the bulk of stellar radio emitters will be very faint (< 1 nanoJy).

3 MULTI-WAVELENGTH PROPERTIES OF MICROJY AND NANOJY RADIO SOURCES

I estimate here the X-ray, optical, and mid-infrared fluxes radio-quiet AGN, SFG, and FR Is should have at the μJy and nanoJy flux density levels. Low-power ellipticals and dwarf galaxies require some discussion.

Balmaverde & Capetti (2006) have studied the multi-wavelength characteristics of very low radio power ellipticals with $10^{19} < P_{5\text{GHz}} < 3 \times 10^{24} \text{ W Hz}^{-1}$ ($\langle P_{5\text{GHz}} \rangle \sim 6 \times 10^{21} \text{ W Hz}^{-1}$). These sources can be considered as miniature radio-galaxies, in the sense that their *nuclear* properties are scaled down versions of those of low-luminosity, FR I radio galaxies. Indeed, if one separates radio galaxies on the basis of their nuclear activity into high-excitation (HERGs) and low-excitation (LERGs) radio-galaxies, almost all FR Is are LERGs and most FR IIs are HERGs, although there is a population of FR II LERGs as well (e.g., Laing et al. 1994). In this scheme, low-power ellipticals could be considered as the natural extension of LERGs to lower radio luminosities. In the following I will then assume that low-power ellipticals have the same multi-wavelength properties as their higher-power relatives, with the obvious caveat that, for the same galaxy optical magnitude they will have a much lower radio emission, and therefore will be characterised by a much lower radio-to-optical flux density ratio. The situation for dwarf galaxies is more complex. In dwarf spheroidals and ellipticals very little, if any, star formation is going on now, although their star formation histories are complex (e.g., Ferguson & Binggeli 1994). Dwarf irregulars appear to be low mass versions of large spirals (e.g., Klein 1986; Leroy et al. 2005), while BCDs fall, on average, at the high star formation rate end (Hunter & Elmegreen 2004).

Since dwarf galaxies are intrinsically weak, our knowledge of their spectral energy distributions (SEDs) is

quite scanty and based on small samples, which are most likely affected by selection effects. My working hypothesis, which is not contradicted by the data (see below), will be that dwarf spheroidals and ellipticals have SEDs similar to those of low-power ellipticals, while dwarf irregulars and BCDs are mini-spirals. As mentioned above, the faint radio sky should be dominated by the star-forming type of dwarfs.

In the following the multi-wavelength fluxes of the various classes of faint radio sources are estimated using three (two for the near-IR band) different methods. Readers not interested in the details should skip directly to Sect. 3.1.3, 3.2.3, and 3.3.2.

3.1 X-ray Band

3.1.1 Typical X-ray-to-radio flux density ratios

Ranalli et al. (2003) have shown that X-ray and radio powers in SFG are strongly correlated, likely because they both trace the star formation rate. Their typical X-ray-to-radio flux ratio is $\langle \log(f_{0.5-2\text{keV}}/S_{1.4\text{GHz}}) \rangle = -17.9 \pm 0.3$ (where the X-ray flux is in c.g.s. units and the radio flux density is in μJy). Although derived for local galaxies, the correlation appears to hold at higher redshifts as well (e.g., Ranalli et al. 2003; Padovani et al. 2009).

Ott, Walter & Brinks (2005) have studied the X-ray properties of eight dwarf galaxies undergoing starburst observed with *Chandra*. I derive $\langle \log(f_{0.5-2\text{keV}}/S_{1.4\text{GHz}}) \rangle \sim -18$ (where I have used observed X-ray fluxes converted to the 0.5 – 2 keV band, taking into account both extended and point source emission, and radio data from the literature), perfectly consistent with the mean value for SFG.

X-ray and radio powers are also correlated in radio-quiet AGN, with a relatively large dispersion (see, e.g., Fig. 13 of Brinkmann et al. 2000). In deriving typical X-ray-to-radio flux density ratios for this class, it is important to keep in mind that, as discussed in Padovani et al. (2009), X-ray selection will tend to favour sources with relatively large X-ray-to-radio flux ratios while the opposite will be true for radio selection. I have used the VLA-CDFS radio-quiet AGN sample selected by Padovani et al. (2009) (and refined by Padovani et al. in preparation) and the X-ray fluxes provided by Tozzi et al. (2009) to obtain a K-corrected value of $\langle \log(f_{0.5-2\text{keV}}/S_{1.4\text{GHz}}) \rangle = -17.2 \pm 0.9$ for radio-selected, radio-quiet AGN. (For $\alpha_x \approx 0.9 - 1.1$, the range covered by (unabsorbed) RQ AGN and spirals, and synchrotron emission ($\alpha_r \sim 0.7$), K-correction effects almost cancel out.) Note that these radio-quiet AGN include both broad-lined (type 1) and narrow-lined (type 2) AGN. Whenever possible, X-ray fluxes were corrected for absorption (see Tozzi et al. 2009, for details). As regards X-ray selected, radio quiet AGN, I use the results of Padovani et al. (2009) on the hard X-ray selected sample of Polletta et al. (2007) ($f_{2-10\text{keV}} > 10^{-14} \text{ erg cm}^{-2} \text{ s}^{-1}$) derived using survival analysis due to the many upper limits on radio flux densities. By converting them to the 0.5 – 2 keV band I obtain a K-corrected mean value $\langle \log(f_{0.5-2\text{keV}}/S_{1.4\text{GHz}}) \rangle \sim -14.8$.

X-ray and radio emission correlate in radio galaxies as well, albeit with a large scatter. Fig. 5 of Padovani et al. (2009) shows that radio galaxies have an X-ray-to-radio power ratio of the same order of that of SFG but smaller than that of quasars. Evans et al. (2006) have studied the X-ray properties of the cores of 22 low-redshift ($z < 0.1$) radio galaxies and find a strong correlation between 1 keV X-ray and 5 GHz radio core powers for low-absorption ($N_H < 5 \times 10^{22} \text{ cm}^{-2}$) radio galaxies, a sub-sample which includes most FR Is. For $\alpha_x = 0.9$ (their average value) and $\alpha_r \sim 0$ (appropriate for radio cores) I get a mean value $\langle \log(f_{0.5-2\text{keV}}/S_{1.4\text{GHz}}) \rangle \sim -18$. One might worry that for more distant sources it will be hard to resolve the nuclear components. I then derived the typical X-ray-to-radio flux density ratio for the FR Is in the AGN catalogue of Padovani et al. (1997) by using total X-ray and radio fluxes, obtaining $\langle \log(f_{0.5-2\text{keV}}/S_{1.4\text{GHz}}) \rangle \approx -19$. In the following I will then adopt the intermediate value $\langle \log(f_{0.5-2\text{keV}}/S_{1.4\text{GHz}}) \rangle \sim -18.5$, noting that even assuming the largest value would not affect any of my conclusions.

Flux density ratios will be largely unaffected by evolution, since this is broadly similar in the X-ray and radio band for SFG (Ranalli, Comastri & Setti 2005) and AGN (e.g., Wall et al. 2005). No information is available on the X-ray evolution of FR Is, which in any case are weak X-ray emitters.

This approach has its limitations. The SFG used by Ranalli et al. (2003) have $S_{1.4\text{GHz}} > 0.1 \text{ Jy}$ and the FR Is studied by Evans et al. (2006) have $S_{5\text{GHz}}(\text{core}) > 0.01 \text{ Jy}$. The derived mean X-ray-to-radio flux density ratios are then used to predict the X-ray fluxes of radio sources in the μJy and nanoJy regime, that is at $\gtrsim 10^4$ times fainter flux density levels. Moreover, these values are likely to be prone to selection effects, which I have tried to take into account in the case of radio-quiet AGN. The latter could be less relevant if these values are based on a strong, physically based correlation, which is likely the case for SFG.

3.1.2 Extrapolation from the VLA-CDFS Sample

An alternative, complementary procedure is to derive the mean X-ray flux for a sample with a relatively faint radio flux density limit and then shift it down to simulate a fainter sample. To this aim, I used the VLA-CDFS sample for which Padovani et al. (2009) (see also Padovani et al., in preparation) provide a classification in SFG and AGN (radio-quiet and radio-loud). Based on their results, most AGN of the radio-loud type are expected to be low-luminosity radio-galaxies, that is FR Is. The flux density limit of the VLA-CDFS survey is not constant but increases with distance from the field centre from a minimum value of $42 \mu\text{Jy}$ (Kellermann et al. 2008). It then follows that low-flux density sources, which, on average, have also the smallest X-ray fluxes, are underrepresented as compared to a sample with a constant limit across the field. To correct for this I have weighted each source by the inverse of the area associated to its flux density. I then divided the mean values of the X-ray flux by 42 to

simulate a sample with $S_{1.4\text{GHz}} \geq 1 \mu\text{Jy}$. Since most SFG and radio-loud AGN are undetected in the X-ray band, only upper limits are available for these two classes. In an hypothetical sample with a radio flux density limit of $1 \mu\text{Jy}$ SFG should have $\langle f_{0.5-2\text{keV}} \rangle < 5 \times 10^{-18} \text{ erg cm}^{-2} \text{ s}^{-1}$, FR Is should have $\langle f_{0.5-2\text{keV}} \rangle < 10^{-17} \text{ erg cm}^{-2} \text{ s}^{-1}$ and radio-quiet AGN should be characterised by $\langle f_{0.5-2\text{keV}} \rangle \sim 2 \times 10^{-17} \text{ erg cm}^{-2} \text{ s}^{-1}$.

3.1.3 X-ray fluxes of faint radio sources

Figure 2 plots 0.5 – 2 keV flux vs. 1.4 GHz radio flux density and shows the loci of X-ray selected and radio-selected, radio-quiet AGN, SFG, and FR Is (Sect. 3.1.1). Note that radio-quiet AGN will span the full range between the two dashed lines in Fig. 2, with radio (X-ray) selection favouring sources with low (high) X-ray-to-radio flux density ratios. The position of these loci with respect to survey limits determines the fraction of sources of a given class detected in one band with counterparts in the other. The figure shows also the expected X-ray fluxes for “typical” radio-quiet AGN, SFG, and FR Is (from the NASA/IPAC Extragalactic Database [NED]) scaled to $1 \mu\text{Jy}$. The mean radio and X-ray flux values, or upper limits, for sources belonging to an hypothetical sample characterised by $S_{1.4\text{GHz}} \geq 1 \mu\text{Jy}$ (Sect. 3.1.2) are also shown. The fact that the three estimates give consistent results is reassuring and shows that we can predict reasonably well the X-ray fluxes of faint radio sources.

The horizontal dot-dashed line at $f_{0.5-2\text{keV}} \sim 2 \times 10^{-17} \text{ erg cm}^{-2} \text{ s}^{-1}$ represents the deepest X-ray data currently available, that is the Chandra Deep Field South 2 Ms Survey (Luo et al. 2008), covering about 0.1 deg^2 . The other horizontal lines indicate, from top to bottom, the limiting fluxes for point sources for surveys to be carried out with eRosita⁹ and the Wide Field X-ray Telescope¹⁰ (WFXT)¹¹. The faintest X-ray flux limit corresponds to the International X-ray Observatory (IXO)¹², which will provide the deepest X-ray view on the Universe for quite some time. IXO will be an observatory type mission, like Chandra, and therefore will not produce large area surveys.

The main message of Fig. 2 is that even the most powerful X-ray missions we are going to have for the next 20 years or so will only detect the counterparts of radio-quiet AGN with radio flux densities down to $\approx 1 \mu\text{Jy}$. The bulk of the μJy population, which is most likely to be made up of SFG, will have X-ray fluxes beyond even the reach of IXO. Same, or possibly even worse, story for FR Is. The situation will obviously be even more critical in the nanoJy regime, where very few radio sources will have an X-ray counterpart in the foreseeable future.

On the positive side, basically all extragalactic sources in the eRosita All-Sky and Wide Surveys and

⁹ <http://www.mpe.mpg.de/heg/www/Projects/EROSITA/-main.html>

¹⁰ <http://wfxt.pha.jhu.edu/>

¹¹ A WFXT-centric version of Fig. 2 has been presented by Padovani (2010)

¹² <http://ixo.gsfc.nasa.gov/>

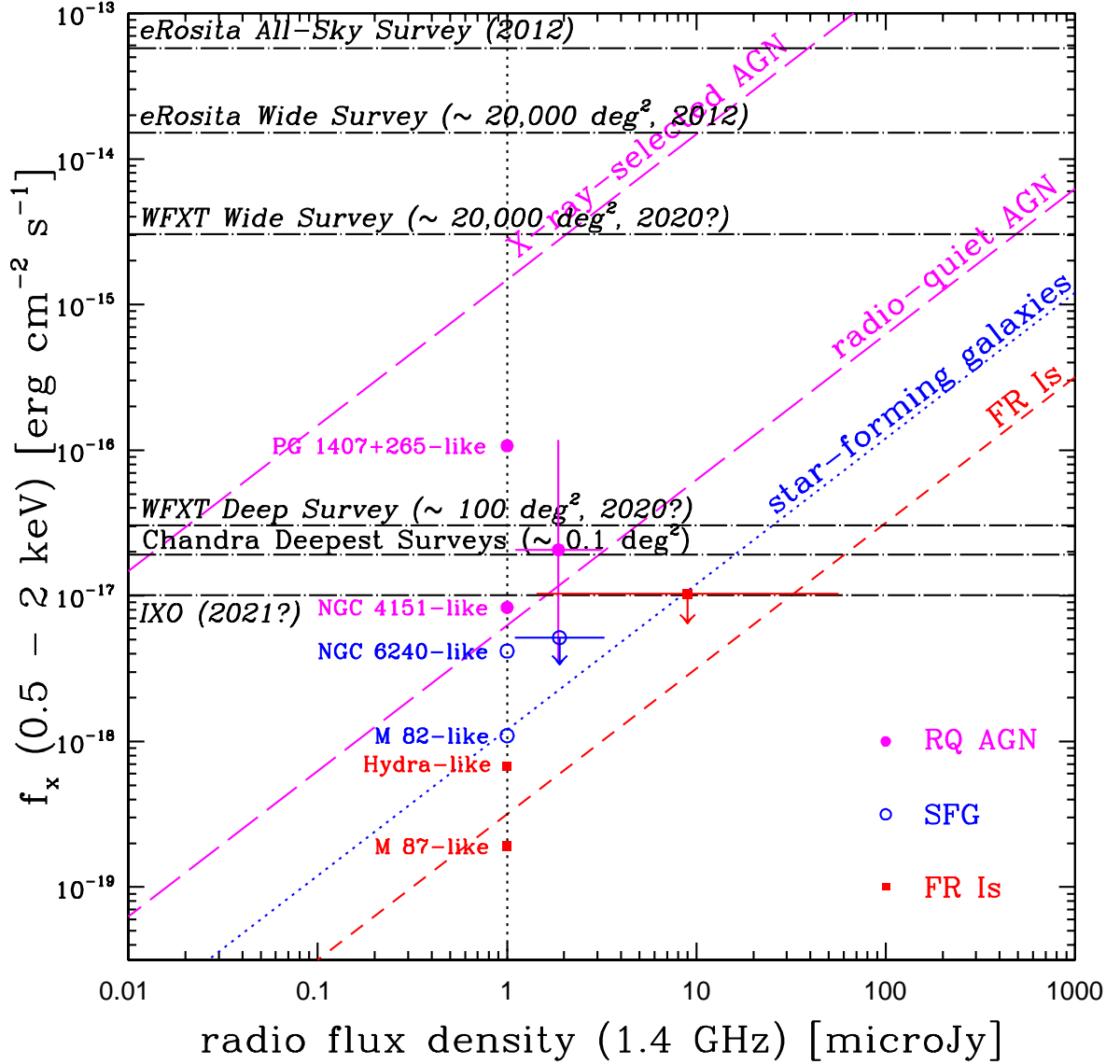


Figure 2. 0.5 – 2 keV X-ray flux vs. the 1.4 GHz radio flux density for faint radio sources. The loci of X-ray selected and radio-selected, radio-quiet AGN (long-dashed lines), SFG (dotted line), and FR Is (short-dashed line) are indicated. The scaled X-ray fluxes of prototypical representatives of the three classes at $S_{1.4\text{GHz}} = 1 \mu\text{Jy}$ are also shown. Finally, the mean radio and X-ray flux values, or upper limits, for sources belonging to an hypothetical sample characterised by $S_{1.4\text{GHz}} \geq 1 \mu\text{Jy}$, as extrapolated from the VLA-CDFS sample, with error bars indicating the standard deviation, are also marked. The horizontal dot-dashed lines indicate the limits of (from top to bottom): the eRosita All-Sky and Wide Surveys, the WFXT Wide and Deep Surveys, Chandra’s deepest surveys, and IXO. Survey areas and launch dates for future missions, or best guesses at the time of writing, are also shown. See text for more details.

WFXT Wide Survey will have an SKA counterpart, as they will have $S_{1.4\text{GHz}} > 1 \mu\text{Jy}$. This should help in the identification work of, for example, the 10 million or so point sources expected in the latter, by also providing very accurate positions. Radio detection of the bulk of the AGN in the WFXT Deep Survey will require much higher (≈ 20 nanoJy) sensitivities. This might be accomplished by the SKA given also the small area of the survey ($\sim 100 \text{ deg}^2$), under the obvious condition that WFXT surveys are carried out in the southern sky.

3.2 Optical Band

3.2.1 Typical radio-to-optical flux density ratios

At variance with the X-ray case, there is in general no apparent correlation between radio and optical powers in extragalactic sources. This is due to the fact that while the radio, far-infrared, and X-ray bands all trace the star formation rate (SFR) (e.g., Kennicutt 1998; Ranalli et al. 2003), the optical band does not, as young stars dominate the ultraviolet continuum. Moreover, as mentioned

in Sect. 2, elliptical galaxies of similar optical power can host radio sources differing by huge amounts in their radio luminosity.

However, SFG and radio-quiet AGN can only reach a reasonably well-defined value of the K-corrected radio-to-optical flux density ratio $R = \log(S_{1.4\text{GHz}}/S_{\text{Rmag}})$, where S_{Rmag} is the R-band flux density (e.g., Machalski & Condon 1999; Padovani et al. 2009). Converting from the values derived for the two classes in the V-band by Padovani et al. (2009) and taking the average one gets for the R-band a maximum value $R \approx 1.4$. Due to K-correction effects (see below), *observed* R values for SFG and radio-quiet AGN can be > 1.4 . It has to be noticed that, while all “classical” radio-loud quasars have $R > 1.4$, this is not the case for many radio-galaxies (e.g., Padovani et al. 2009), which can extend to $R < 1.4$. Indeed, as mentioned above, low-power ellipticals will have lower R values than FR Is.

The absolute SFR in star-forming galaxies spans a very large range, from $\sim 20 M_{\odot} \text{ yr}^{-1}$ in gas-rich spirals to $\sim 100 M_{\odot} \text{ yr}^{-1}$ in optically selected starburst galaxies and up to $\sim 1000 M_{\odot} \text{ yr}^{-1}$ in the most luminous IR starbursts (Kennicutt 1998). Therefore, for the same optical magnitude “normal” spirals will be characterised by lower radio emission than starbursts, and therefore will have a smaller radio-to-optical flux density ratio. To better quantify this I will define as a “normal”, non-starburst source a galaxy with an SFR $< 10 M_{\odot} \text{ yr}^{-1}$, which is the maximum value reached by local Uppsala Galaxy Catalogue (UGC) galaxies (James et al. 2004). Converting this to a radio power following the calibration of Sargsyan & Wedman (2009), which agrees very well with that based on polycyclic aromatic hydrocarbons (PAH), translates to $P_{1.4\text{GHz}} < 8.4 \times 10^{21} \text{ W Hz}^{-1}$. SFG in the VLA-CDFS sample below this value have $R \lesssim 0.3$ (and $z \lesssim 0.2$). Padovani et al. (2009) have also shown that R decreases with decreasing $P_{1.4\text{GHz}}$ for the spirals and irregulars in their sample. From Fig. 1 of Condon (1989) (converting from his cosmology) I derive $R \lesssim 0.1$ for $P_{1.4\text{GHz}} \sim 8 \times 10^{21} \text{ W Hz}^{-1}$ for optically bright ($B_T \leq 12$) spirals and irregulars; lower radio powers have smaller R values.

Dwarf galaxies have also low flux density ratios and are in fact underrepresented in radio samples (Van Deyne et al. 2004). From the mean values given by Leroy et al. (2005) I get $R \approx -0.6$ (converting to my notation), while Fig. 9 of Leon et al. (2008) shows that $R < -0.8$ for $M_B \sim -17$. Even BCDs, which are the most star-forming amongst dwarfs, are characterised by $R \approx -0.2$ (Hunt, Bianchi & Maiolino 2005).

In the optical band the K-correction is quite important. For example, at $z \sim 1$, the mean redshift of the VLA-CDFS sample, it reaches ~ 1 magnitude for Sbc galaxies and ~ 2 magnitudes for ellipticals (e.g., Coleman et al. 1980). These values should be compared to the factor ~ 1.2 in flux (equivalent to ~ 0.2 magnitudes) expected in the radio band (for $\alpha_r \sim 0.7$). Moreover, absorption by the intergalactic medium will also further decrease the optical flux. It then follows that the derived magnitudes are very robust lower limits. As was the case for the X-ray band, flux density ratios will be largely unaffected by evolution, since

this is broadly similar in the optical and radio band for SFG (Ranalli, Comastri & Setti 2005) and powerful AGN (Wall et al. 2005). For FR Is and low-power ellipticals, however, the evolutionary correction in the optical band can be quite important (Poggianti 1997). This, coupled to the almost absent radio evolution (Sect. 2), could imply a decrease in radio-to-optical flux density ratios for these classes at high redshifts.

3.2.2 Extrapolation from the VLA-CDFS Sample

The best estimate of the optical magnitudes of faint radio sources is obtained by scaling those of a sample with a relatively faint radio flux density limit. Using the same procedure as for the X-ray band (Sect. 3.1.2), I added to the $\langle R_{\text{mag}} \rangle$ of the VLA-CDFS sources $2.5 \times \log 42$ to simulate a sample with $S_{1.4\text{GHz}} \geq 1 \mu\text{Jy}$. Correcting for the non-uniform flux density limit as done before (Sect. 3.1.2), SFG in this hypothetical sample should have $\langle R_{\text{mag}} \rangle \sim 26.3$, radio-quiet AGN should have $\langle R_{\text{mag}} \rangle \sim 28.2$ and radio-loud AGN (mostly low-luminosity radio-galaxies) should have $\langle R_{\text{mag}} \rangle \sim 27.3$. Note that $\sim 85\%$ of the SFG in the VLA-CDFS sample have radio powers above the “normal” spiral limit and so are mostly of the starburst type.

3.2.3 Optical magnitudes of faint radio sources

Figure 3 plots R_{mag} vs. 1.4 GHz radio flux density and shows: 1. the expected R_{mag} for “typical” radio-quiet AGN, SFG (starbursts, spirals, and dwarfs), and FR Is (from NED) scaled to $1 \mu\text{Jy}$; 2. the maximum value for SFG and the approximate dividing line between radio-loud and radio-quiet AGN (diagonal dashed line; see Sect. 3.2.1). SFG and radio-quiet AGN are expected to populate the top left part of the diagram; 3. the mean radio and R_{mag} values for sources belonging to an hypothetical sample characterised by $S_{1.4\text{GHz}} \geq 1 \mu\text{Jy}$ (Sect. 3.2.2).

The three methods give consistent results, which is reassuring and shows that we have a reasonable handle on the magnitudes of faint radio sources. The scaled R_{mag} for radio-quiet AGN are fainter than those derived for “typical” sources and are beyond the $R = 1.4$ line. This is because these sources have the highest redshifts in the VLA-CDFS sample, and therefore their observed magnitudes are more affected by K-correction effects.

The horizontal dot-dashed line at $R_{\text{mag}} \sim 29.3$ represents the limit of the deepest optical data currently available, the Hubble UDF (Beckwith et al. 2006), covering about 11 arcmin^2 . The other horizontal lines indicate, from top to bottom, the limiting magnitudes for the Panoramic Survey Telescope and Rapid Response System (PAN-STARRS)¹³, which from Hawaii will survey about 3/4 of the sky down to $R_{\text{mag}} \sim 26$ during 10 years of operation and the Large Synoptic Survey Telescope (LSST)¹⁴, which will be located in Chile and will provide a survey of about half the sky down to $R_{\text{mag}} \sim 27.5$ during 10 years

¹³ <http://pan-starrs.ifa.hawaii.edu/>

¹⁴ <http://www.lsst.org>

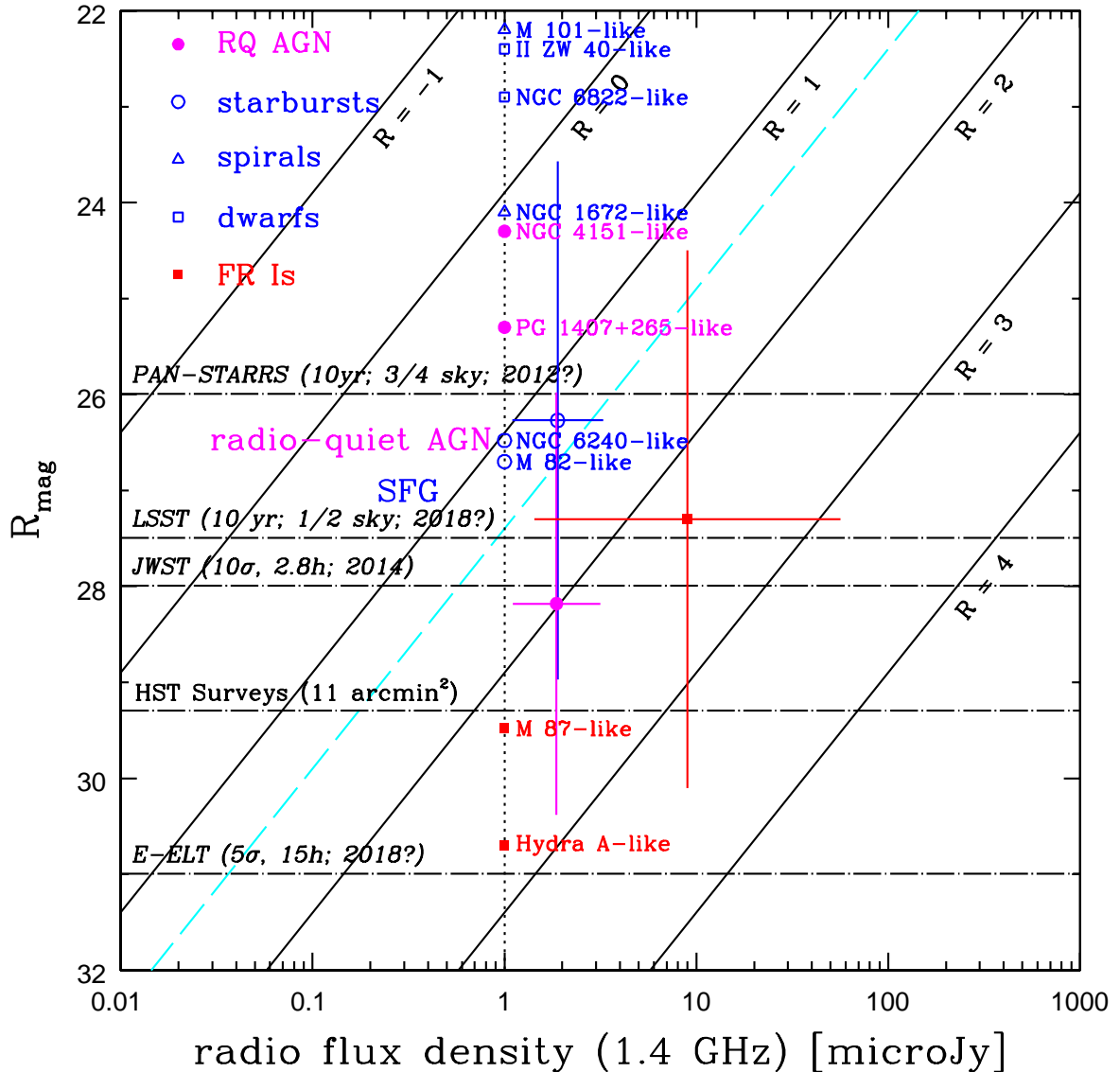


Figure 3. R_{mag} vs. the 1.4 GHz radio flux density for faint radio sources. Diagonal lines represent different values of $R = \log(S_{1.4\text{GHz}}/S_{R_{\text{mag}}})$, ranging from -1 (top) to 4 (bottom). The diagonal dashed line at $R = 1.4$ indicates the maximum value for SFG and the approximate dividing line between radio-loud and radio-quiet AGN, with SFG and radio-quiet AGN expected to populate the top left part of the diagram. The scaled R magnitudes of prototypical representatives of the three classes at $S_{1.4\text{GHz}} = 1 \mu\text{Jy}$ are also shown, with SFG split into starbursts, spirals, and dwarfs. Finally, the mean radio and R_{mag} values for sources belonging to an hypothetical sample characterised by $S_{1.4\text{GHz}} \geq 1 \mu\text{Jy}$, as extrapolated from the VLA-CDFS sample, with error bars indicating the standard deviation, are also marked. The horizontal dot-dashed lines indicate the approximate point-source limits of (from top to bottom): PAN-STARRS, LSST, JWST, the deepest Hubble Space Telescope surveys, and the E-ELT. Survey areas (for LSST and PAN-STARRS), S/N ratios and exposure times (for the E-ELT and JWST) and operation/launch dates for future missions, or best guesses at the time of writing, are also shown. See text for more details.

of operation. Further below there are the limiting magnitudes for point sources for the James Webb Space Telescope (JWST)¹⁵ and for the European Extremely Large Telescope¹⁶ (E-ELT)¹⁷ for the given signal-to-noise (S/N)

ratios and exposure times¹⁸. Both these telescopes will operate in observatory mode. It is important to keep in mind

largest mirror (42 m in diameter) amongst the three very large telescopes being planned. The other two are the Thirty Meter Telescope (TMT; <http://www.tmt.org/>) and the Giant Magellan Telescope (GMT; <http://www.gmto.org/>).

¹⁸ The JWST limit comes from the JWST Web pages. The E-ELT limit was derived from the E-ELT Exposure Time Cal-

¹⁵ <http://www.stsci.edu/jwst/>

¹⁶ <http://www.eso.org/sci/facilities/eelt/>

¹⁷ I am using the E-ELT as an example because it has the

that all of these limits are only approximate, as none of these telescopes are in operation yet.

Given the progression towards lower R values going from (non-dwarf) starbursts, to spirals, and to BCDs and dwarf irregulars (Sect. 3.2.1), the typical magnitudes of faint radio sources at a given flux density will depend critically on which of these SFG sub-classes dominates the counts.

The contribution of “normal” spirals to faint radio number counts is not well known. Hopkins et al. (2000), by converting the optical LF to a radio LF adopting a constant ratio $P_{1.4\text{GHz}}/L_B = 1/3$, predict that normal galaxies will outnumber starbursts at $S_{1.4\text{GHz}} \sim 1 \mu\text{Jy}$. Since R is a function of radio power, this assumption is too simplistic. I have used a different approach based on the SFR division introduced above (Sect. 3.2.1). Namely, I have split the SFG LF of Sadler et al. (2002) into two at $P_{1.4\text{GHz}} = 8.4 \times 10^{21} \text{ W Hz}^{-1}$ and evaluated the number counts assuming the evolution of Hopkins (2004). The result is that “normal” spirals should be more numerous than starbursts for $S_{1.4\text{GHz}} \lesssim 5 \mu\text{Jy}$.

Are dwarf galaxies also going to be relevant at the flux densities of interest here ($\gtrsim 10 \text{ nanoJy}$)? Although we do not have any information on their radio LF, one can make an educated guess by converting their optical LF. Leon et al. (2008) find that radio and optical power for Sb – Sc galaxies extending down to $M_B \sim -16$ scale linearly; the scaling factor is consistent with the mean values for the dwarf galaxies studied by Leroy et al. (2005), which reach $M_B \sim -14$. I have then transformed the dwarf LF of Blanton et al. (2005) to a radio LF, which covers the range $10^{18} \lesssim P_{1.4\text{GHz}} \lesssim 3 \times 10^{20} \text{ W Hz}^{-1}$. Assuming the same evolution as SFG and integrating as done above to $z_{\text{max}} = 3$, one then finds that dwarfs outnumber non-dwarf SFG at $S_{1.4\text{GHz}} \lesssim 20 \text{ nanoJy}$. This result is quite robust towards extrapolations of the optical LF to fainter magnitudes ($M_r \sim -10$) with the same slope ($\alpha = -1.52$), while a steepening of the LF ($\alpha = -2.0$) would lead to an increase in the flux density below which dwarfs dominate by a factor ~ 3 . Note also that any evolution smaller than the assumed one would push further down the contribution of dwarf galaxies at a given flux density. However, the range in radio power covered by this radio LF does not extend to the values reached by some BCDs ($P_{1.4\text{GHz}} > 5 \times 10^{20} \text{ W Hz}^{-1}$; e.g., Hunt, Bianchi & Maiolino 2005; Sargsyan & Wedman 2009). I have then multiplied the scaling factor by $10^{0.5}$ to take into account the somewhat larger radio-to-optical flux density ratio of BCDs (see Sect. 3.2.1), with the result that dwarfs should outnumber non-dwarf SFG at $S_{1.4\text{GHz}} \lesssim 0.3 \mu\text{Jy}$. Since not all dwarfs are BCDs, dwarf galaxies will become the most numerous constituents of the radio sky at flux densities in the likely range $20 \text{ nanoJy} \lesssim S_{1.4\text{GHz}} \lesssim 300 \text{ nanoJy}$.

Fig. 3 shows that, down to $1 \mu\text{Jy}$, most starburst-like SFG and radio-quiet AGN should be detected by the LSST, that is they will have a counterpart in a large area survey. To be more specific, based on the

VLA-CDFS extrapolation, $\sim 66\%$ of starburst galaxies with $S_{1.4\text{GHz}} \geq 1 \mu\text{Jy}$ should have $R_{\text{mag}} < 27.5$. This number represents an upper limit because by scaling the VLA-CDFS magnitudes I have assumed that the mean redshift is unchanged, while Padovani et al. (2009) have found a strong correlation between redshift and magnitude. Therefore, K-correction effects will be larger and observed magnitudes will be fainter. On the other hand, “normal” spirals should outnumber starbursts for $S_{1.4\text{GHz}} \lesssim 5 \mu\text{Jy}$. If even distant spirals are characterised by rest-frame $R \lesssim 0.1 - 0.3$, as is the case for local sources (Sect. 3.2.1), then μJy sources could be ≈ 2 magnitudes brighter than expected in the case of starbursts and therefore within reach of PAN-STARRS and certainly of the LSST. For fainter radio samples optical magnitudes should get fainter, unless dwarf galaxies, with their low R values, become dominant, which would lead yet to another “brightening”. For example, for $R \approx -0.5$ and $S_{1.4\text{GHz}} \approx 100 \text{ nanoJy}$, $R_{\text{mag}} \approx 25$.

FR Is have on average larger R values but also higher radio flux densities, so their mean magnitude in an hypothetical $S_{1.4\text{GHz}} \geq 1 \mu\text{Jy}$ sample is brighter than those for “typical” sources with $S_{1.4\text{GHz}} = 1 \mu\text{Jy}$, although the R values are similar. Low-power ellipticals, however, will have smaller R and therefore brighter magnitudes.

Sources having $R_{\text{mag}} > 27.5$ will obviously be within reach of JWST and ELTs, which however will be covering a relatively small field of view (up to a few arcmin²). Depending on the actual relative fraction of starbursts, spirals, and dwarfs, these observatories could be the main (only?) facilities to secure optical counterparts of nanoJy radio sources.

To address the question of what fraction of sources in the LSST and PAN-STARRS surveys will have an SKA counterpart requires a knowledge of the radio properties of very faint optical sources, which at present we do not possess. Nevertheless, one can make some educated guesses. The UDF number counts of Beckwith et al. (2006) show that for $z_{\text{AB}} \lesssim 26$ the surface density is $\sim 3 \times 10^5 \text{ deg}^{-2}$, which implies, based on Fig. 1, that the majority of the objects beyond this limit are star-forming systems. SFG in the VLA-CDFS sample have observed $R \approx 1.3$, which means $S_{1.4\text{GHz}} \approx 3 \mu\text{Jy}$ and $\approx 70 \text{ nanoJy}$ at $R_{\text{mag}} \sim 26$ and ~ 27.5 respectively, that is within reach of the SKA. Optical selection however will be biased towards smaller R and therefore fainter radio flux densities. More importantly, spirals and dwarfs, which might be the most numerous sub-classes, with their lower R values will have fainter radio flux densities for a given magnitude. As regards the small minority of radio-quiet AGN, they can reach $R \sim -1.5$ in the AGN catalogue of Padovani et al. (1997), which would imply extremely low radio flux densities even for PAN-STARRS. However, White et al. (2007), by stacking FIRST radio images for $\sim 40,000$ SDSS quasars, have shown that R increases with magnitude, which would imply higher radio flux densities at faint magnitudes. In summary, the bulk of LSST and PAN-STARRS sources *might not* have radio flux densities within reach of the SKA, but at this point in time one cannot be more specific.

culator (ETC) using the Laser-Tomography/Multi-Conjugate Adaptive Optics option.

3.3 Mid-Infrared Band

3.3.1 Typical mid-infrared-to-radio flux density ratios

The infrared and radio emission are strongly and linearly correlated in SFG, defining what is known as the “IR-radio relation” (e. g., Sargent et al. 2010, and references therein). The most recent determination of the so-called (K-corrected) q_{24} parameter, based on the COSMOS field and using an IR/radio-selected sample to reduce selection biases, is $q_{24} = \log(S_{24\mu\text{m}}/S_{1.4\text{GHz}}) = 1.26 \pm 0.13$ (Sargent et al. 2010). As mentioned above (Sect. 3.1.1), radio selection will favour objects with larger radio flux densities, and therefore smaller q_{24} , but given the tightness of the relation the decrease is only ~ 0.3 (based on Tab. 3 of Sargent et al. (2010)). BCDs also appear to have q parameters globally consistent with those of SFG (Hunt, Bianchi & Maiolino 2005), even though Bell (2003) argues that both the IR and radio luminosities of dwarf galaxies significantly underestimate the SFR by similar amounts. Radio-quiet AGN have q_{24} values similar to those of SFG, while radio-loud ones have much smaller ones. For this band we cannot extrapolate from the VLA-CDFS sample since most of the sources are undetected in the 24 μm band in publicly available catalogues.

Evolution in the mid-infrared and radio band is broadly similar for SFG (Ranalli, Comastri & Setti 2005) and AGN (e.g., Weedman & Houck 2009). Therefore, typical flux density ratios will be largely unaffected by it. No information is available on the mid-infrared evolution of FR Is, which in any case are very weak IR emitters.

3.3.2 Mid-Infrared flux densities of faint radio sources

Figure 4 plots the 24 μm vs. 1.4 GHz radio flux density and shows the expected $f_{24\mu\text{m}}$ for “typical” radio-quiet AGN and SFG (from NED), scaled to 1 μJy (the values for two “typical” dwarf galaxies are fully consistent with these and are not included for clarity) and the locus of SFG and radio-quiet AGN (Sect. 3.3.1). The two methods give perfectly consistent results. The two “typical” FR Is have $f_{24\mu\text{m}} \sim 0.2 - 0.8$ nanoJy and are therefore way off the plot.

The two top horizontal dot-dashed lines represent the point-source limits for the Wide-field Infrared Survey Explorer (WISE)¹⁹ and AKARI²⁰. Both are performing all-sky infrared surveys. However, I give the AKARI limit for pointing mode as the survey limit for the band closest to the one of interest (18 μm) is off the plot (120 mJy). The horizontal line at $f_{24\mu\text{m}} \sim 40$ μJy indicates the deepest mid-infrared data currently available, that is the Spitzer observations of the GOODS/FIDEL field (B  thermin et al. 2010), covering about 0.23 deg². The bottom two horizontal lines denote the limiting flux densities for point sources for JWST and the SPace Infrared telescope for Cosmology and Astrophysics (SPICA)²¹ for

the given S/N ratios and exposure times. Both these telescope will operate in observatory mode. These two limits are only approximate, as none of these telescopes are in operation yet.

Figure 4 shows that most SFG and radio-quiet AGN should be detected by JWST down to ~ 1 μJy and by SPICA down to ~ 100 nanoJy. Both telescopes will be covering a relatively small field of view (up to ≈ 15 arcmin²). Only a tiny fraction of μJy and nanoJy SFG and radio quiet AGN will have a counterpart in an all-sky infrared surveys. As regards FR Is, they will be largely undetected even by SPICA.

On the other hand, all extragalactic sources in the WISE and AKARI all-sky surveys will easily have an SKA counterpart, as they will be characterised by $S_{1.4\text{GHz}} \gtrsim 100$ μJy .

4 REDSHIFTS OF FAINT RADIO SOURCES

A vital component in the identification of astronomical sources is redshift, which allows powers to be estimated and LF’s to be derived. Figure 5 plots R_{mag} vs. 1.4 GHz radio flux density but, at variance from Fig. 3, the marked limits refer to spectroscopic or photometric redshifts.

The top horizontal dot-dashed line represents the current limiting magnitude for “classical” photometric redshifts, which reach $R_{\text{mag}} \approx 24$ and $z \approx 1.5$ (e.g., Mainieri et al. 2008); photometric redshifts for special classes of sources, e.g., $z \sim 7$ drop-outs can be derived with HST down to $Y_{\text{AB}} \approx 28$ (Bouwens et al. 2010). Long exposures ($\sim 10\text{h}$) with 8/10 m telescopes can secure spectroscopic redshifts *in the case of strong emission lines* down to $R_{\text{mag}} \approx 26$, so this value represents a hard limit. Finally, indicative limiting magnitudes for obtaining spectra for point sources with the E-ELT and JWST are also shown²².

Fig. 5 shows that, down to 1 μJy , only approximately half of the starburst-like SFG will be within reach of 8/10 m telescopes in terms of obtaining a spectroscopic redshift. To be more specific, based on the VLA-CDFS extrapolation, $\sim 50\%$ of starburst galaxies with $S_{1.4\text{GHz}} \geq 1$ μJy should have $R_{\text{mag}} > 26$ and $\sim 60\%$ will be above $R_{\text{mag}} = 25$, probably a more realistic limit for a spectrum. As discussed above (Sect. 3.2.3), these fractions are robust upper limits. On the other hand, spiral, and maybe dwarf galaxies, should be more common than starbursts at μJy and nano-Jy levels, respectively, which would lead to brighter magnitudes, thereby making the job of deriving a redshift easier. Future facilities like the E-ELT and JWST will obviously allow the determination of spectroscopic redshifts for fainter ($R_{\text{mag}} > 26$)

²² The JWST limit refers to a resolution of 1,000 and $\lambda = 1$ μm and comes from the JWST Web pages. The E-ELT limits apply to a resolution of 1,000, the R band, and was derived from the E-ELT ETC using the Laser-Tomography/Multi-Conjugate Adaptive Optics option. Since the choice of instruments for the E-ELT has not been finalised yet, these limits are *very* preliminary. Note that in both cases the magnitudes refer to the continuum: the presence of emission lines will obviously lead to shorter exposure times.

¹⁹ <http://wise.ssl.berkeley.edu/>

²⁰ <http://www.ir.isas.jaxa.jp/ASTRO-F/>

²¹ <http://www.ir.isas.jaxa.jp/SPICA/>

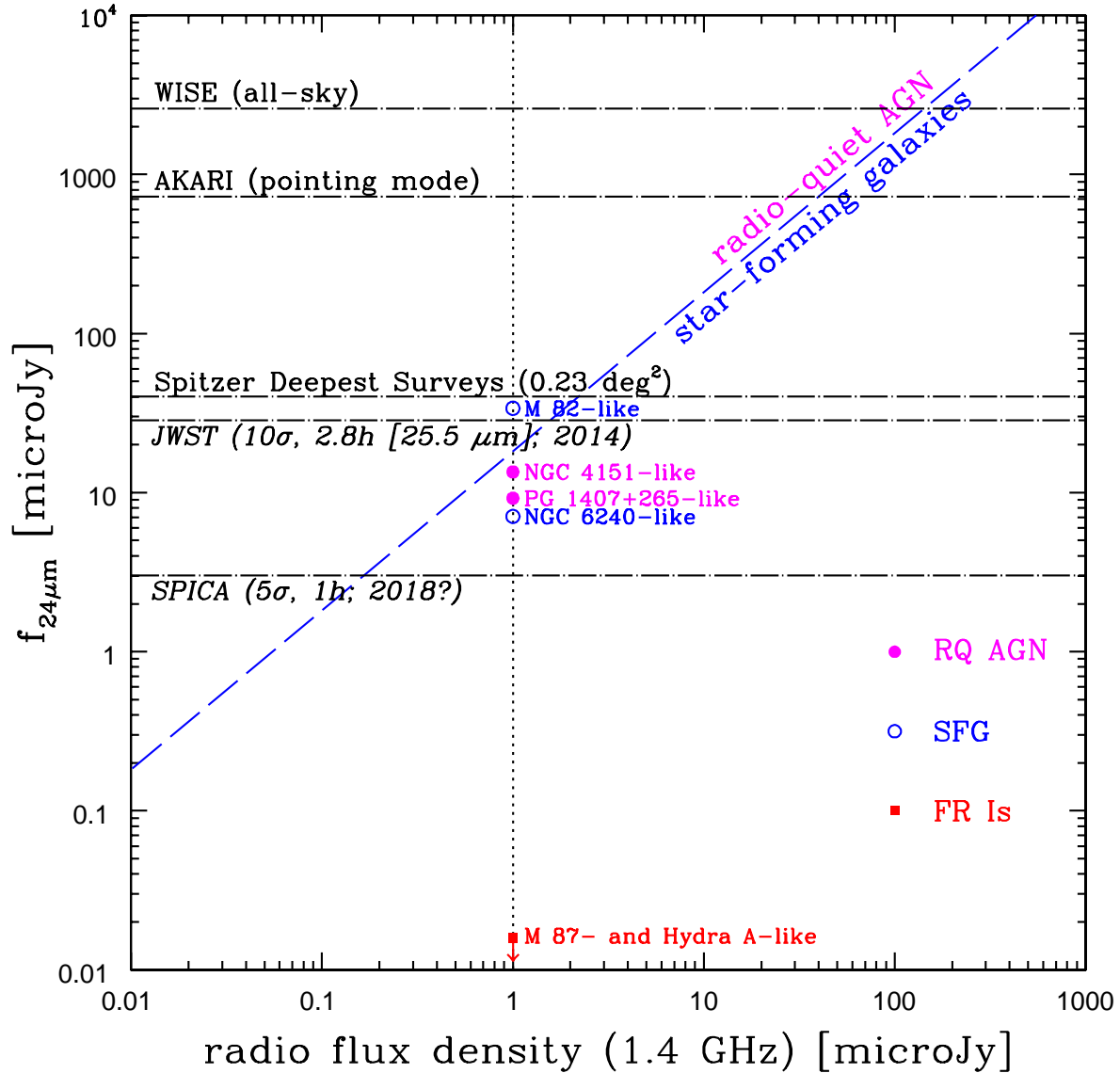


Figure 4. $24\mu\text{m}$ flux density vs. the 1.4 GHz radio flux density for faint radio sources. The diagonal dashed line represents the locus of SFG and radio-quiet AGN based on the “IR-radio relation”. The scaled IR flux densities of prototypical representatives of the three classes at $S_{1.4\text{GHz}} = 1 \mu\text{Jy}$ are also shown, with FR Is being so faint as to be actually off the plot at $f_{24\mu\text{m}} \sim 0.2 - 0.8$ nanoJy. The horizontal dot-dashed lines indicate the approximate point-source limits of (from top to bottom): WISE, AKARI (pointing mode), the deepest Spitzer surveys, JWST, and SPICA. Launch dates for future missions, or best guesses at the time of writing, are also shown. See text for more details.

objects, albeit with relatively long exposures. It might be also reasonable to suppose that the LSST will reach the required accuracy to determine photometric redshifts for sources one magnitude brighter than its 10 yr survey limit, thereby reaching $R_{\text{mag}} \approx 26.5$. However, both LSST and PAN-STARRS will work with photometric systems with ~ 6 optical broadband filters, similar to those traditionally used in astronomy, which means that they will be more prone to color-redshift degeneracies than systems using a larger number of narrower filters (Benítez et al. 2009). Since the reddest filter is going to

be in the y -band ($\sim 1.05 \mu\text{m}$), this will also limit the maximum achievable redshift.

Note that the magnitude limits of the current deepest large-area spectroscopic surveys are $r \leq 17.8$ (galaxies) and $i \leq 19.1$ (quasars) for the SDSS²³ and $b_J \leq 20.85$ for the 2dF QSO redshift survey²⁴.

In summary, many of the $S_{1.4\text{GHz}} \geq 1 \mu\text{Jy}$ sources might be too faint for 8/10 m telescopes to be able to provide a redshift and the situation might get worse at

²³ <http://www.sdss.org/dr7/>

²⁴ <http://www.2dfquasar.org/>

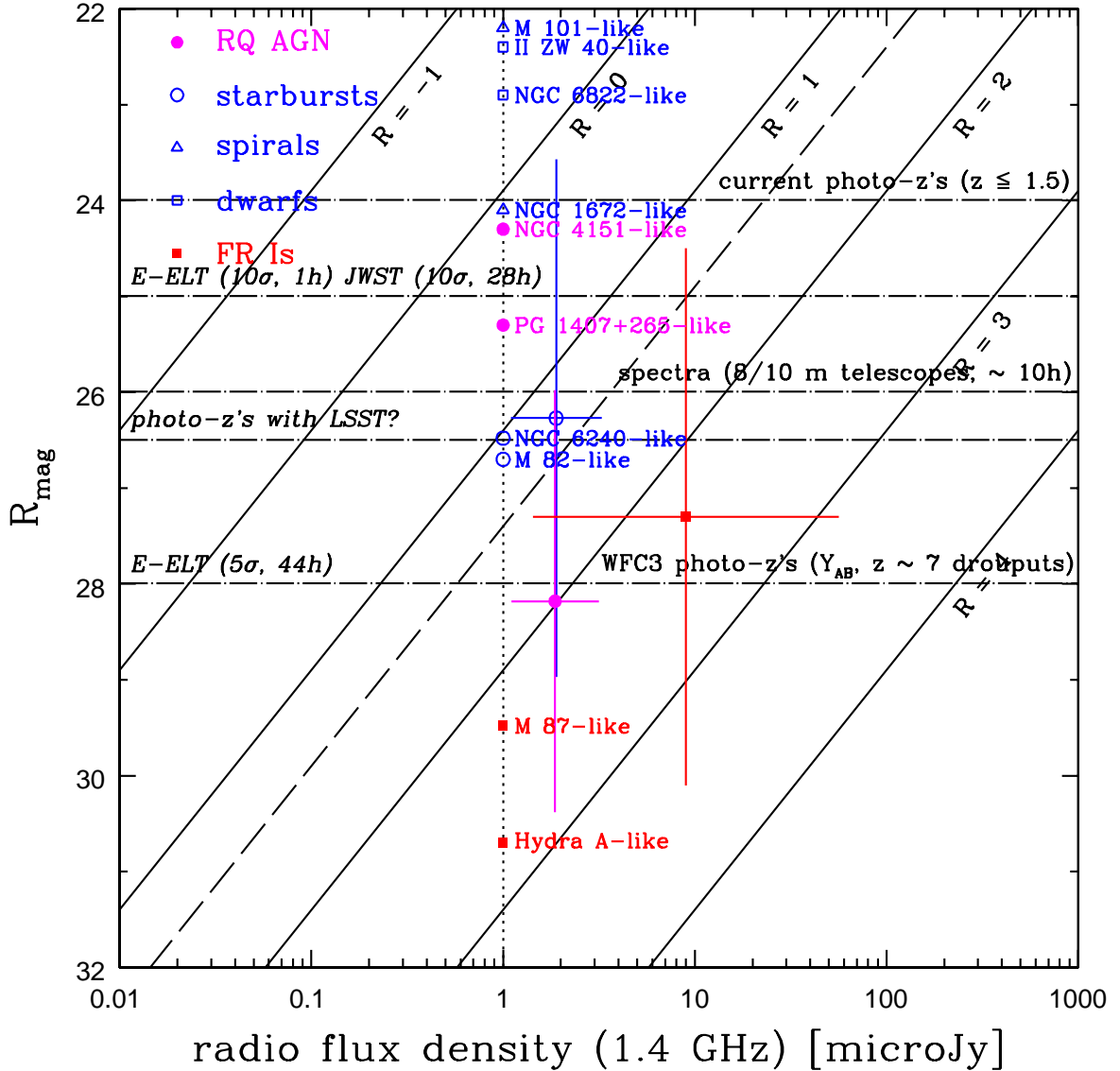


Figure 5. R_{mag} vs. the 1.4 GHz radio flux density for faint radio sources. Diagonal lines represent different values of $R = \log(S_{1.4\text{GHz}}/S_{R_{\text{mag}}})$, ranging from -1 (top) to 4 (bottom). The diagonal dashed line at $R = 1.4$ indicates the maximum value for SFG and the approximate dividing line between radio-loud and radio-quiet AGN, with SFG and radio-quiet AGN expected to populate the top left part of the diagram. The scaled R magnitudes of prototypical representatives of the three classes at $S_{1.4\text{GHz}} = 1 \mu\text{Jy}$ are also shown, with SFG split into starbursts, spirals, and dwarfs. Finally, the mean radio and R_{mag} values for sources belonging to an hypothetical sample characterised by $S_{1.4\text{GHz}} \geq 1 \mu\text{Jy}$, as extrapolated from the VLA-CDFS sample, are also marked. The horizontal dot-dashed lines indicate the approximate limiting magnitudes to derive photometric and spectroscopic redshifts. From top to bottom: the current limit for photometric redshifts, the JWST and an E-ELT limit (for the given S/N ratios and exposure times), the faintest magnitude for which a spectroscopic redshift can be obtained with 8/10 m telescopes, a possible limit for photometric redshifts with the LSST, a fainter E-ELT limit, and the limit of photometric redshifts for $z \sim 7$ drop-outs with the Wide Field Camera 3 (WFC3) on board HST. See text for more details.

fainter flux densities, unless dwarf galaxies take over. This means that JWST and the ELTs might be the main facilities to secure redshifts of μJy radio sources. But even they could have problems in the nanoJy regime.

5 DISCUSSION

The simple approach employed in this paper suggests that (non-dwarf) SFG play a very important role in the sub- μJy sky, something which had been already realised by many authors. What is new here is that also low-power ($P_{1.4\text{GHz}} < 10^{20} \text{ W Hz}^{-1}$) ellipticals but especially dwarf galaxies are very relevant, with the latter

very likely being the most important constituent of the faint radio sky. The arguments I have used to reach this conclusions appear quite robust. Indeed, by limiting the integration to $z_{\max} = 3$ for lack of information, the derived values on the surface densities of these classes are lower limits. Christlein et al. (2009) have recently used a new maximum likelihood method to derive a LF down to $M_r \approx -14$, which displays a faint end slope $\alpha = -1.62$ steeper than the LF of Blanton et al. (2005) I have used for my calculations (which has $\alpha = -1.52$). The number (and therefore surface) density of dwarf galaxies is then probably even higher than I have assumed.

The radio, far-infrared, and X-ray bands all trace star formation, which implies relatively tight relationships between these three bands. This means that we can reasonably predict the mid-infrared and X-ray properties of SFG with faint radio flux densities. The situation is different in the optical band, which is dominated by emission from evolved stars. Since “normal” spirals and dwarf galaxies have radio-to-optical flux density ratios smaller than starbursts because of their lower star formation rate, they will be brighter in the optical band at a given radio flux density ratio. The optical properties of faint radio sources will then depend on the population mix of starbursts, spirals, and dwarf galaxies, which at present cannot be determined very accurately. Given our ignorance of the radio LF and evolution of dwarf galaxies, in fact, it is not straightforward to predict at which flux densities they will become the dominant population. By converting the optical LF to a radio LF, under the assumption (not inconsistent with the available data) of a linear proportionality between the two powers and of an evolution similar to that of SFG, dwarfs should outnumber non-dwarf SFG in the 20 – 300 nanoJy range. However, this cannot be the whole story, as the estimated radio LF reaches only $P_{1.4\text{GHz}} \sim 10^{21} \text{ W Hz}^{-1}$, while there are BCDs with $P_{1.4\text{GHz}}$ up to $\approx 10^{22} \text{ W Hz}^{-1}$ (Sargsyan & Wedman 2009). There has then to be a high-power component of the LF, which will translate into a higher number of sources at high flux densities, which at present cannot be quantified.

Can the two “new” populations be relevant also for the radio background? Singal et al. (2010) have concluded that the main background contributors have to be faint (sub- μJy) radio sources and suggested these to be ordinary star-forming galaxies at $z > 1$ characterised by an evolving radio far-infrared correlation, which increases toward the radio loud with redshift (but see Sargent et al. (2010) for evidence that the local radio far-infrared relation still holds up to $z \sim 5$). Massardi et al. (2010) (see also Padovani et al., in preparation) have shown that population synthesis models of the radio sky, which currently involve only “classical” radio sources, fail to explain by a factor of a few (see their Fig. 9) the very recent background measurements of Fixsen et al. (2010). Since background emission from a population of objects is equal to $\int SN(S)dS$ (where $N(S)$ are the differential counts), which is a combination of surface and flux density, the right mix of numbers and fluxes are needed to provide a relevant contribution. Therefore, while low-power ellipticals, which are both faint and not that numerous, are most likely unimportant, for dwarf galaxies the situation

is less obvious. On one hand, even with the largest scaling factor used in Sect. 3.2.3, dwarf galaxies account for only $\approx 8\%$ of the sub-mJy background. But on the other hand, the radio LF is not known and, as discussed above, the radio number counts of dwarf galaxies could well be higher.

The determination of the surface densities for all classes of radio sources allows us also to determine the *intrinsic* ratio between radio-loud and radio-quiet AGN. The surface density of SSRQs and FSRQs combined is $\sim 6.3 \text{ deg}^{-2}$, while that of radio-quiet, broad-lined AGN is $\approx 5 \times 10^3 \text{ deg}^{-2}$, since unabsorbed AGN are supposed to make up $\sim 1/5$ of the total (Gilli et al. 2007). This translates to a radio-loud fraction in broad-lined AGN $\approx 0.1\%$. If one considers both broad- and narrow-lined sources, which means including also FR IIs in the radio-loud class and all radio-quiet AGN, one gets a similar fraction $\approx 0.2\%$. These numbers are much smaller than the oft-quoted value of $\approx 10 - 20\%$. However, it has been known for some time that the radio-loud fraction drops with decreasing optical luminosity (Padovani 1993). Very recently, Jiang et al. (2007) have shown that the fraction of radio-loud quasars at $z = 0.5$ declines from 24% to 6% as luminosity decreases from $M_{2500} = -26$ to -22 , while at $M_{2500} = -26$ this fractions declines from 24% to 4% as redshift increases from 0.5 to 3. Both these results suggest that the intrinsic, global ratio has to be $\lesssim 5\%$. But if the radio-loud fraction were this large, the radio-loud quasar surface density should be $\approx 250 \text{ deg}^{-2}$, that is ~ 40 times larger than estimated here and also ~ 5 larger than that of FR IIs, which are supposed to be the parent population of both SSRQs and FSRQs. Scaling up the FR II surface density as well to avoid this paradox, one would end up having more FR IIs than FR Is, which would not make any sense at all, since FR IIs are more powerful. In short, the surface densities derived in this paper point to an AGN radio-loud fraction much smaller than normally derived. This difference is likely to be ascribed to two factors: a) the usually quoted value has been obtained for bright, optically selected samples (Kellermann et al. 1989), which include radio-loud quasars with their optical flux boosted by relativistic beaming (Goldschmidt et al. 1999), which artificially increases their fraction; b) radio-loud AGN are on average more powerful than radio-quiet ones (e.g., Zamfir, Sulentic & Marziani 2008). When one reaches the very faint end of the optical LF only radio-quiet AGN will be present and therefore the integrated radio-loud fraction will be quite small. In other words, the usually quoted value refers to the bright part of the LF and, when integrated over the full range of powers, the resulting radio-loud fraction is much smaller. The second factor is likely to be the most relevant one.

The issue of source confusion goes beyond the scope of this paper. I will just point out that Windhorst et al. (2008) have shown that ultra-deep radio and optical surveys may slowly approach the natural confusion limit, where objects start to overlap with their neighbours due to their finite sizes and not because of the finite instrumental resolution, which causes the instrumental confusion limit. Based on the model of Windhorst (2003), confusion will not be a problem for the SKA if source sizes are $\lesssim 1.6''$ at $S_{1.4\text{GHz}} = 1 \mu\text{Jy}$ (or $\lesssim 0.25''$ at $S_{1.4\text{GHz}} = 10$

nanoJy) and the instrumental resolution is commensurate (Windhorst et al. 2008). However, since Windhorst (2003) did not include radio-quiet AGN, low-power ellipticals, or dwarf galaxies, confusion limits are bound to be higher. Indeed, Owen & Morrison (2008), based on the relatively flat number counts derived from their deep radio data, have suggested that the natural confusion limit may be reached near $1 \mu\text{Jy}$.

6 CONCLUSIONS

I have used a simple method to work out the source population of the sub- μJy sky, which relies on estimating the smallest flux density and the largest surface density for all classes of radio sources. These two parameters can be derived quite robustly from the local minimum radio power and number of sources per unit volume, maximum redshift, and luminosity and density evolution. I have then estimated for the first time the X-ray, optical, and mid-infrared fluxes these faint radio sources are likely to have by using prototypical sources, typical flux density ratios, and extrapolations from the VLA-CDFS sample. Prognosticating these multi-wavelength properties is extremely relevant for the identification of μJy and nanoJy radio sources and to maximise the synergy between the SKA and its pathfinders with future missions in bands other than the radio. My main results can be summarised as follows:

(1) The sub- μJy sky should consist of radio-quiet AGN ($\approx 2 \times 10^4 \text{ deg}^{-2}$) and star-forming galaxies ($\approx 3 \times 10^6 \text{ deg}^{-2}$), both of which should get to $S_{1.4\text{GHz}} \approx 0.1 - 1 \text{ nanoJy}$. In agreement with previous studies, I find that classical, powerful radio sources, that is radio quasars and FR IIs, do not make it to sub- μJy flux densities and reach $S_{1.4\text{GHz}} \approx 0.1 \text{ mJy}$, with BL Lacs and FR Is getting to the $\approx 1 - 10 \mu\text{Jy}$ level.

(2) The *intrinsic* fraction of radio-loud AGN, integrated over the whole bolometric luminosity function, is $\approx 0.1 - 0.2\%$, that is about two orders of magnitude smaller than the oft-quoted value of $\approx 10 - 20\%$. The latter value refers only to the bright part of the optical luminosity function and is also biased because of the likely flux boosting in radio-loud quasars due to relativistic beaming.

(3) Two “new” populations, which have not been considered previously, appear to be very relevant: low-power ($P_{1.4\text{GHz}} < 10^{20} \text{ W Hz}^{-1}$) ellipticals and dwarf galaxies. Using the available (scanty) information, the former should reach similar flux and surface densities as radio-quiet AGN, while the latter could easily be the most numerous component of the faint radio sky ($\gtrsim 5 \times 10^6 \text{ deg}^{-2}$), with flux densities as low as $\approx 1 \text{ nanoJy}$. Since most galaxies at the faint end of the LF are blue, most dwarfs in the Universe (and therefore most radio sources) should be of the star-forming type. While low-power ellipticals are most likely unimportant contributors to the radio background, the verdict is still open for dwarf galaxies. This issue is quite important also in light of the very recent background measurements reported by the ARCADE 2 collaboration (Fixsen et al. 2010).

(4) The bulk of the μJy population, which is then most probably going to be made up of star-forming galaxies, is likely to have X-ray fluxes beyond the reach of all currently planned X-ray missions, including IXO. The same applies to FR Is. Even IXO will only detect radio-quiet AGN with radio flux densities $\gtrsim 1 \mu\text{Jy}$. The situation will obviously be worse in the nanoJy regime, where very few radio sources will have an X-ray counterpart in the foreseeable future. On the other hand, basically all extragalactic sources in the eRosita All-Sky and Wide Surveys and WEXT Wide Survey will have an SKA counterpart, as they will be characterised by $S_{1.4\text{GHz}} > 1 \mu\text{Jy}$. This will help in the identification of, for example, the 10 million or so point sources expected in the latter, by also providing very accurate positions.

(5) In the mid-infrared most star-forming galaxies and radio-quiet AGN should be detected by JWST down to radio flux densities $\sim 1 \mu\text{Jy}$ and by SPICA down to $\sim 100 \text{ nanoJy}$, while FR Is will be largely undetected even by SPICA. Both telescopes will however be covering a relatively small field of view. Only a minute fraction of μJy and nanoJy star-forming galaxies and radio quiet AGN will have a counterpart in current all-sky infrared surveys (WISE and AKARI). On the positive side, all extragalactic sources in the WISE and AKARI all-sky surveys will easily have an SKA counterpart, as they will be characterised by $S_{1.4\text{GHz}} \gtrsim 100 \mu\text{Jy}$.

(6) Since the radio, far-infrared, and X-ray emission all trace star formation, this implies relatively tight relationships between these three bands, which in turn means that we can reasonably predict the mid-infrared and X-ray properties of star-forming galaxies with faint radio flux densities. The situation is different in the optical band, where evolved stars dominate. Objects characterised by higher star formation rates will have larger radio-to-optical flux density ratios, which means fainter magnitudes for a given radio flux density. The typical magnitudes of the optical counterparts of faint radio sources depend then on which type of star-forming galaxy (starburst, spiral, or dwarf) will be predominant. Moreover, in the optical band K-correction and intergalactic absorption effects are important and will result in fainter than expected magnitudes. Assuming a maximum value of star formation rate for “normal” spirals, which translates to a maximum radio power, I estimate that these sources should outnumber starbursts for $S_{1.4\text{GHz}} \lesssim 5 \mu\text{Jy}$. If even distant spirals are characterised by relatively low rest-frame radio-to-optical flux density ratios, then most μJy sources should be detected by PAN-STARRS and certainly by the LSST. At fainter radio flux densities optical magnitudes should also get fainter, unless dwarf galaxies, with their lower radio-to-optical flux density ratios, become dominant. Depending on the relative fraction of starbursts, spirals, and dwarfs, JWST and especially the ELTs could be the main, or perhaps even the only, facilities capable of securing optical counterparts of nanoJy radio sources. On the other hand, and for the same reasons discussed above, the bulk of PAN-STARRS and LSST sources might not have radio flux densities within reach of the SKA.

(7) As regards redshifts, the same complications described above apply, since the optical band is still in-

volved. Within the same uncertainties, then, many of the sources with $S_{1.4\text{GHz}} \geq 1 \mu\text{Jy}$ might be too faint for 8/10 m telescopes to be able to provide a redshift determination and the situation might get worse at fainter flux densities, unless dwarf galaxies are prevalent. This means that JWST and particularly the ELTs might be the primary facilities to secure redshifts of μJy radio sources. But even they could have problems in the nanoJy regime.

In summary, the SKA and its pathfinders will have a huge impact on a number of open problems in extragalactic astronomy. Apart from the “obvious” study of star-forming galaxies in their various incarnations and “classical” radio sources, these include also less evident ones, ranging from what makes a galaxy radio-loud (through the study of low-power ellipticals), to why most AGN are radio-quiet (by selecting large samples independent of obscuration), to the incidence and evolution of dwarf galaxies (by providing a “cleaner” radio selection, which might by-pass the surface brightness problems of optical samples), to the resolution of the radio background.

Identifying faint radio sources, however, will not be easy. On large areas of the sky the SKA will be quite alone in the multi-wavelength arena, with the likely exception of the optical band and even there probably only down to $\approx 1 \mu\text{Jy}$. SPICA, JWST, and especially the ELTs will be a match for the SKA but only on small areas and above $0.1 - 1 \mu\text{Jy}$. At fainter flux densities one might have to resort to “radio only” information, that is HI redshifts, size, morphology, spectral index, etc., although I think this will not be sufficient. On the bright side, most sources from currently planned all-sky surveys, with the likely exception of the optical ones, will have an SKA counterpart.

ACKNOWLEDGMENTS

The idea for this paper came to me while preparing a talk for the SKA 2010 meeting held in Manchester, UK, in March 2010. My thanks to the organisers of that meeting for inviting me. I also thank Michael Hilker, Ken Kellermann, Jochen Liske, Vincenzo Mainieri, Nicola Menci, Steffen Mieske, and Piero Rosati for useful discussions, and the anonymous referee for his/her suggestions. This research has made use of the NASA/IPAC Extragalactic Database (NED) which is operated by the Jet Propulsion Laboratory, California Institute of Technology, under contract with the National Aeronautics and Space Administration and of NASA’s Astrophysics Data System (ADS) Bibliographic Services.

REFERENCES

- Balmaverde B., Capetti A., 2006, *A&A*, 447, 97
 Becker R. H., White R. L., Helfand D. J., 1995, *ApJ*, 450, 559
 Beckwith S. V. W., et al., 2006, *ApJ*, 132, 1729
 Bell E. F., 2003, *ApJ*, 586, 794
 Bell E. F., et al., 2004, *ApJ*, 608, 752
 Benítez N., et al., 2009, *ApJ*, 692, L5
 Béthermin M., Dole H., Beelen A., Aussel H., 2010, *A&A*, 512, A78
 Blanton M. R., Lupton R. H., Schlegel D. J., Strauss M. A., Brinkmann J., Fukugita M., Loveday J., 2005, *ApJ*, 631, 208
 Bondi M., et al., 2008, *ApJ*, 681, 1129
 Bouwens R. J., et al., 2010, *ApJL*, 709, L133
 Brinkmann W., Laurent-Muehleisen S. A., Voges W., Siebert J., Becker R. H., Brotherton M. S., White R. L., Gregg M. D., 2000, *A&A*, 356, 445
 Capetti A., Kharb P., Axon D. J., Merritt D., Baldi R. D., 2009, *AJ*, 138, 1990
 Cattaneo A., et al., 2009, *Nature*, 460, 213
 Christlein D., Gawiser E., Marchesini D., Padilla N., 2009, *MNRAS*, 400, 429
 Cimatti A., Daddi E., Renzini A., 2006, *A&A*, 453, L29
 Coleman G. D., Wu C.-C., Weedman D. W., 1980, *ApJS*, 43, 393
 Condon J. J., 1989, *ApJ*, 338, 13
 Condon J. J., Cotton W. D., Greisen E. W., Yin Q. F., Perley R. A., Taylor G. B., Broderick J. J., 1998, *AJ*, 115, 169
 Cooray A., 2005, *MNRAS*, 364, 303
 de Lapparent V., Galaz G., Bardelli S., Arnouts S., 2003, *A&A*, 404, 831
 de Zotti G., Ricci R., Mesa D., Silva L., Mazzotta P., Toffolatti L., González-Nuevo J., 2005, *A&A*, 431, 893
 Evans D. A., Worrall D. M., Hardcastle M. J., Kraft R. P., Birkinshaw M., 2006, *ApJ*, 642, 96
 Ferguson H. C., Sandage A., 1991, *AJ*, 101, 765
 Ferguson H. C., Binggeli B., 1994, *A&ARv*, 6, 67
 Fixsen D. J., et al., 2010, *ApJ*, submitted (arXiv:0901.0555)
 Fomalont E., et al., 2002, *AJ*, 123, 2402
 Gendre M. A., Best P. N., Wall J. V., 2010, *MNRAS*, 450, 1719
 Gilli R., Comastri A., Hasinger G., 2007, *A&A*, 463, 79
 Goldschmidt P., Kukula M. J., Miller L., Dunlop J. S., 1999, *ApJ*, 511, 612
 Hasinger G., Miyaji T., Schmidt M., 2005, *A&A*, 441, 417
 Hopkins A., Windhorst R., Cram L., Ekers R., 2000, *Experimental Astronomy*, 10, 419
 Hopkins A. M., 2004, *ApJ*, 615, 209
 Hunt L., Bianchi S., Maiolino R., 2005, *A&A*, 434, 849
 Hunter D. A., Elmegreen B. G., 2004, *AJ*, 128, 2170
 Jackson C. A., 2004, *New Astronomy Reviews*, 48, 1187
 James P. A., et al., 2004, *A&A*, 414, 23
 Jarvis M. J., Rawlings S., 2004, *New Astronomy Reviews*, 48, 1173
 Jiang L., Fan X., Ivezić Ž., Richards G. T., Schneider D. P., Strauss M. A., Kelly B. C., 2007, *ApJ*, 656, 680
 Kellermann K. I., Sramek R., Schmidt M., Shaffer D. B., Green R., 1989, *AJ*, 98, 1195
 Kellermann K. I., Fomalont E. B., Mainieri V., Padovani P., Rosati P., Shaver P., Tozzi P., Miller N., 2008, *ApJS*, 179, 71
 Kennicutt R. C., Jr., 1998, *ARA&A*, 36, 189
 Klein U., 1986, *A&A*, 168, 65
 Kriek M., van der Wel A., van Dokkum P. G., Franx M., Illingworth G. D., 2008, *ApJ*, 682, 896

- Laing R. A., Jenkins C. R., Wall J. V., Unger S. W., 1994, *ASPC*, 54, 201
- Leon S., et al., 2008, *A&A*, 485, 475
- Leroy A., Bolatto A. D., Simon J. D., Blitz L., 2005, *ApJ*, 625, 763
- Luo B., et al., 2008, *ApJS*, 179, 19
- Machalski J., Condon J. J., 1999, *ApJS*, 123, 41
- Mainieri V., et al., 2008, *ApJS*, 179, 95
- Massardi M., Bonaldi A., Negrello M., Ricciardi S., Raccanelli A., de Zotti G., 2010, *MNRAS*, 404, 532
- Massaro E., Giommi P., Leto C., Marchegiani P., Maselli A., Perri M., Piranomonte S., Sclavi S., 2009, *A&A*, 495, 691
- Merloni A., Rudnick G., Di Matteo T., 2008, in *Relativistic Astrophysics Legacy and Cosmology - Einstein's*, ESO Astrophysics Symposia. Springer-Verlag Berlin Heidelberg, 158
- Miller N. A., Hornschemeier A. E., Mobasher B., Bridges T. J., Hudson M. J., Marzke R. O., Smith R. J., 2009, *AJ*, 137, 4450
- Morganti R., et al., 2009, in *Panoramic Radio Astronomy: Wide-field 1-2 GHz research on galaxy evolution*, Gröningen, The Netherlands, June 2009, (arXiv:1001.2384)
- Ott J., Walter F., Brinks E., 2005, *MNRAS*, 358, 1423
- Owen F. N., Morrison G. E., 2008, *AJ*, 136, 1889
- Padovani P., 1993, *MNRAS*, 263, 461
- Padovani P., Giommi P., Fiore F., 1997, in *From the Micro- to the Mega-Parsec*, ed. A. Comastri, T. Venturi, & M. Bellazzini, *Memorie della Società Astronomica Italiana*, 68, 147
- Padovani P., Giommi P., Landt H., Perlman E. S., 2007, *ApJ*, 662, 182
- Padovani P., et al., 2009, *ApJ*, 694, 235
- Padovani P., 2010, in *The Wide Field X-ray Telescope workshop*, Bologna, Nov. 25-26, 2009, to appear in the proceedings (arXiv:1004.4536)
- Poggianti B. M., 1997, *A&AS*, 122, 399
- Polletta M., et al., 2007, *ApJ*, 663, 81
- Ranalli P., Comastri A., Setti G., 2003, *A&A*, 399, 39
- Ranalli P., Comastri A., Setti G., 2005, *A&A*, 440, 23
- Rush B., Malkan M. A., Edelson R. A., 1996, *ApJ*, 473, 130
- Sadler E. M., Jenkins C. R., Kotanyi C. G., 1989, *MNRAS*, 240, 591
- Sadler E. M., et al., 2002, *MNRAS*, 329, 227
- Sajina A., Lacy M., Scott D. 2005, *ApJ*, 621, 256
- Salimbeni S., et al., 2008, *A&A*, 477, 763
- Sargent M. T., et al., 2010, *ApJS*, 186, 341
- Sargsyan L. A., Weedman, D. W., 2009, *ApJ*, 701, 1398
- Seaquist E. R., 1997, in *High-Sensitivity Radio Astronomy*, ed. D. Jackson. University of Manchester, Manchester, 23
- Seymour N., et al., 2008, *MNRAS*, 386, 1695
- Singal J., Stawarz L., Lawrence A., Petrosian V., 2010, *MNRAS*, in press (arXiv:0909.1997)
- Smolčić V., et al., 2008, *ApJS*, 177, 14
- Strazzullo V., Pannella M., Owen F. N., Bender R., Morrison G. E., Wang W.-H., Shupe D. L., 2010, *ApJ*, 714, 1305
- Tozzi P., et al., 2009, *ApJ*, 698, 740
- Urry C. M., Padovani P., 1995, *PASP*, 107, 803
- Van Duyne J., Beckerman E., Salzer J. J., Gronwall C., Thuan T.X., Condon J. J., Frattare L. M., 2004, *AJ*, 127, 1959
- Wall J. V., Jackson C. A., Shaver P. A., Hook I. M., Kellermann K. I., 2005, *A&A*, 434, 133
- Weedman D. W., Houck J. R., 2009, *ApJ*, 698, 1682
- White R. L., Helfand D. J., Becker R. H., Glikman E., de Vries W., 2007, *ApJ*, 654, 99
- White S. M., 2004, *New Astronomy Reviews*, 48, 1319
- Wilman R. J., et al., 2008, *MNRAS*, 388, 1335
- Windhorst R. A., 2003, *New Astronomy Reviews*, 47, 357
- Windhorst R. A., Cohen S. H., Hathi N. P., Jansen R. A., Ryan R. E., 2008, *AIPC*, 1035, 318
- Zamfir S., Sulentic J. W., Marziani P., 2008, *MNRAS*, 387, 856